

# Development and Optimization of Cassava (*Manihot Esculenta*) Peeling Machine

B. O. Udoji<sup>1</sup>; T. K. Kaankuka<sup>2</sup>; J. O. Awulu<sup>3</sup>; S. S. Igila<sup>4</sup>  
<sup>1,2,3,4</sup>Joseph Sarwuan Tarka University Makurdi Benue State Nigeria

**Abstract:-** The conventional cassava peeling methods are inefficient, time-consuming, and labor-intensive. This study aimed to create an enhanced cassava peeling machine with minimal flesh loss. The machine design includes components like a hopper, shafts, bearings, an electric motor, and a v belt connected to a pulley that drives the brush-equipped shaft. This locally sourced and fabricated machine, designed for 50kg of cassava tubers, was tested at operational speeds of 380, 420, and 460 rpm and retention times of 4, 6, and 8 minutes, optimizing the effects of machine speeds and peeling times on peeling efficiency using I-optimal Response Surface Experimental Design with a mean separation at  $P < 0.05$ . Results pertaining to tuber properties, such as angle of repose, peel thickness, moisture content, peel penetration force, bulk density, and coefficient of friction, were utilized in the machine's design. The machine achieved maximum peeling efficiency of 74% at a speed of 380m/s when operated for 6 minutes. At this optimal efficiency, the machine reached an optimal throughput capacity of 171.4kg/h, with a 21% flesh loss, a peeling weight proportion of 25.8%, and minimal tuber damage (3.3%). The desirability, which signifies the extent to which these optimal values align with the optimization goal, was 0.83 (83%). In essence, this machine significantly advances cassava peeling mechanization.

**Keywords:-** Cassava, Optimization, Peeling Machine AD Development

## I. INTRODUCTION

Cassava (*manihot esculenta*) referred to as cassava, manioc, and tapioca, belongs to the Euphorbiaceae (spurge) family and is primarily found in South America (ARS, 2015). Cultivated as an annual crop in tropical and subtropical regions, cassava is renowned for its woody shrub nature and its edible starchy tuberous root, serving as a significant source of carbohydrates (Oriole and Raji, 2013). It is the third-largest contributor to food carbohydrates in the tropics, following rice and maize (APS, 2015). Cassava is a major staple food in developing world, providing a basic diet for over half a billion people (FAO, 2015), it is one of the most drought tolerant crops, capable of growing on marginal soils. Nigeria is the world's largest producer of cassava followed by Brazil (Uthman, 2011). There are many varieties of cassava which are Tropical Manihot Specie TMS 90257, TMS 50395, TMS 30001, TMS 82/00661, TMS 84537, National Roots NR41044, NR 8082, they are distinguished based on many criteria relating to the structural features of the plant, other

features are tuber shapes, earliness of maturity, yields and its content of cyanogenic glycoside concentrations respectively (Martin and Ejike, 2018). In the processing of cassava, various unit operations are involved, including peeling, grating, boiling, drying, milling, and sifting (FAO, 2005). Cassava peeling, a critical initial operation, is considered a laborious task, with traditional methods involving hand peeling after harvesting and cleaning. Cassava peels consist of two layers, namely the outer layer (periderm) and the inner layer (cortex) (Adetan et al., 2005). Although peeling has been practiced since the inception of cassava cultivation, the tools used have evolved from stone and wooden flints to contemporary household knives. The quality of the end product is significantly affected by the peeling operation, particularly concerning unwanted contents. In cases where cassava is utilized for animal feed, peeling may be deemed unnecessary (Adetunji and Quadri, 2011). Manual peeling, primarily achieved by hand, is time-consuming and energy-intensive. Skilled manual peeling typically yields around 25kg/hr, with a loss of 25-30% of weight in peels (FAO, 2005). Mechanization of the cassava peeling process is crucial for increased production rates, particularly in commercial farms or industries. Challenges arise due to variations in cassava root properties such as weight, size, shape, thickness, texture, and adhesion strength to the flesh, making it difficult to design a universal cassava peeling machine (Aghetoye, 2005; Adetan et al., 2006). Numerous attempts have been made to develop cassava peeling machines, but the common issue is their tendency to reduce tubers to a uniform cylindrical shape, resulting in the wastage of useful flesh. Therefore, there is a need to design and develop a cassava peeling machine capable of accommodating different sizes of cassava.

## II. MATERIALS AND METHOD

### A. General

A cassava peeling machine was designed, constructed, evaluated and optimized. Cassava tuber properties were determined to know its physical and mechanical behavior. Cassava properties determined were length, width, size and shape, angle of repose, moisture content, penetration force and shearing strength. 20-30 kg of unpeeled cassava tubers were used to evaluate the machine at a varying speed, peeling time was observed and recorded using a stop watch for these varying speeds of 380, 420 and 460. A peeling time of 4, 6 and 8 minutes was observed and recorded using a stop watch for these varying speeds. A model was generated for optimization; Quadratic models were chosen for operational parameters tested.

### B. Materials for Performance Test

Cassava tubers (TMS 30001) of different sizes were harvested fresh and washed from farm in Makurdi.

### C. Materials for Construction

The materials and tools used for this work includes the flat iron, angle iron, sheet metal, stainless steel, ball bearings, drilling machine, chain and sprocket, belt and pulley, synthetic brushes, shafts, measurement tape (with millimeter graduation), lath machine and milling machine was used during the construction of the machine.

### D. Physical and Mechanical Properties of Cassava Tuber Relevant to Peeling

#### ➤ Determination of Moisture Content

Moisture content for randomly selected and cleaned cassava tubers were determined. The cleaned tubers were slice transversely with a knife. The moisture content was determined by oven drying the samples at 105°C for 24 hrs. This was done for 3 different samples. The moisture content was calculated using the formula by Ndirika and Oyeleke (2006) as given in equation 1.

$$M_c (wb) \% = \frac{w_w - w_d}{w_w} \times \frac{100}{1} \quad (1)$$

Where;

$W_w$  = weight of wet sample (g),

$W_d$  = weight of dried sample (g),

$M_c$  = moisture content wet basis (%).

#### ➤ Determination of Axial Dimensions of Cassava Tuber

The procedure for the determination of principal dimensions was adopted as describe by Prasad *et al.* (2010). The three principal dimensions namely length (L), width (W), and thickness (T) were measured on 10 tubers of cassava using a digital vernier calliper with accuracy of  $\pm 0.01$  mm.

#### • Geometric Mean Diameter

The geometric mean diameter (Dg) of the cassava tuber was evaluated using equation 2 given as:

$$D_g = (LWT)^{\frac{1}{3}} \quad (2)$$

Where;

$D_g$  = Geometric mean diameter (mm)

$L$  = Length of cassava tuber (mm)

$W$  = Width of cassava tuber (mm)

$T$  = Thickness of cassava tuber (mm)

#### • Determination of Arithmetic Mean Diameter

The arithmetic mean diameter (Da) of the cassava was calculated using equation 3 given by Baryeh and Mangope (2002).

$$D_a = \frac{L+W+T}{3} \quad (3)$$

Where;

$D_a$  = Arithmetic mean diameter (mm)

#### ➤ Determination of Surface Area of Cassava Tuber

The surface area (Sa) of cassava was obtained from equation 4 given by Baryeh and Mandope (2002).

$$S_a = \pi(D_g)^2 \quad (4)$$

Where;

$S_a$  = Surface area of cassava tuber (mm<sup>2</sup>)

#### ➤ Determination of Bulk Density, True Density and Porosity of Cassava Tuber

- Bulk density was determined by weighing the tubers packed in a container of known volume. A digital weighing balance of  $\pm 0.01$ g accuracy was used to determine the mass of cassava tubers in the container. Equation 5 as given by Waziri and Mittal (1983) was used to determine the bulk density of the cassava tubers in 3 replications.

$$\rho_b = \frac{M_{mp}}{V_k} \quad (5)$$

Where;

$\rho_b$  = Bulk density of cassava, kg/m<sup>3</sup>

$M_{mp}$  = Mass of packed cassava tuber, kg

$V_k$  = Known volume of container, m<sup>3</sup>

- True density or real density can be defined as the ratio of the mass to the volume occupied by the mass. The determination of true density was determined by weighing the mass of cassava tuber to be peeled in grams using weigh scale. The volume was calculated in cubic centimetre by multiplying length, height and breath; divide the mass of the cassava tubers being weighed by the volume to determine the true density (Callahan, 2018).
- True density was determined using equation 6 given as:

$$\rho_t = \frac{M}{V_u} \quad (6)$$

Where;

$\rho_t$  = True density, kg/m<sup>3</sup>

$V_u$  = Volume of cassava, m<sup>3</sup>

- Porosity ( $\delta$ ) of bulk tuber is defined as the ratio of inter-tuber spaces to the total shape occupied by tuber; it was calculated using equation 7 given by Tunde-Akintunde and Akintunde, (2007).

$$\delta = \left(1 - \frac{\rho_b}{\rho_t}\right) \times 100 \% \quad (7)$$

Where;

$\delta$  = Porosity, (%)

$\rho_t$  = True density, kg/m<sup>3</sup>

$\rho_b$  = Bulk density, kg/m<sup>3</sup>

➤ *Determination of the Tuber Circumference*

The circumference of the tuber was determined by measuring 10 cassava tubers with a vernier calliper in its widest point.

➤ *Determination of Thickness of Peel*

The tuber was cut transversely in the central point and peeled; the peels were measured separately with a precision Vernier calliper. The accuracy (precision) of the instrument was of 0.01 mm and this was done for 10 cassava tubers.

*E. Design of Machine Components*

The following components of the cassava peeling machine were designed; hopper, belt drive, shaft, chain and sprocket, peeling drum, shaft bearing, discharge chute and frame. In designing these components, the physical and mechanical properties of cassava tuber were considered.

➤ *Hopper Design*

The cassava peeling machine has one hopper which has its base welded to the frame by arc welding as shown in figure 3. The hopper was designed to have a trapezoidal shape with its end projecting into the peeling chamber. It was inclined at the angle of 79.6° to the peeling chamber, to allow free fall of

cassava tuber into the peeling chamber. The 79.6° corresponds to the determined angle of repose of cassava tuber on metal by Nwachukwu and Simonyan, (2015).

❖ *Volume of Hopper*

Volume of hopper was determined from equation 8 (Oberg et al., 2004)

$$V_f = \frac{H_h}{3} (A_1 + A_2 + \sqrt{A_1 \times A_2}) \tag{8}$$

$$A_1 = L_f \times B_1 = 1 \times 0.4 = 0.4 \text{ m}$$

$$A_2 = L_f \times B_2 = 1 \times 0.202 = 0.202 \text{ m}$$

$$H_h = 0.278 \text{ m (based on design calculations)}$$

$$B_1 = \text{Breadth of the top frustum} = 0.4 \text{ m}$$

$$B_2 = \text{Breadth of the base frustum} = 0.202 \text{ m}$$

$$L_f = \text{length of frustum} = 1 \text{ m}$$

Where;

$V_f$  = Volume of frustum, m<sup>3</sup>

$A_1$  = Area of the top of the frustum = 0.4 m<sup>2</sup>

$A_2$  = Area of the base of the frustum = 0.202 m<sup>2</sup>

$$V_f = \frac{1}{3} (0.4 + 0.202 + \sqrt{0.4 \times 0.202}) = 0.29 \approx 0.3 \text{ m}^3$$

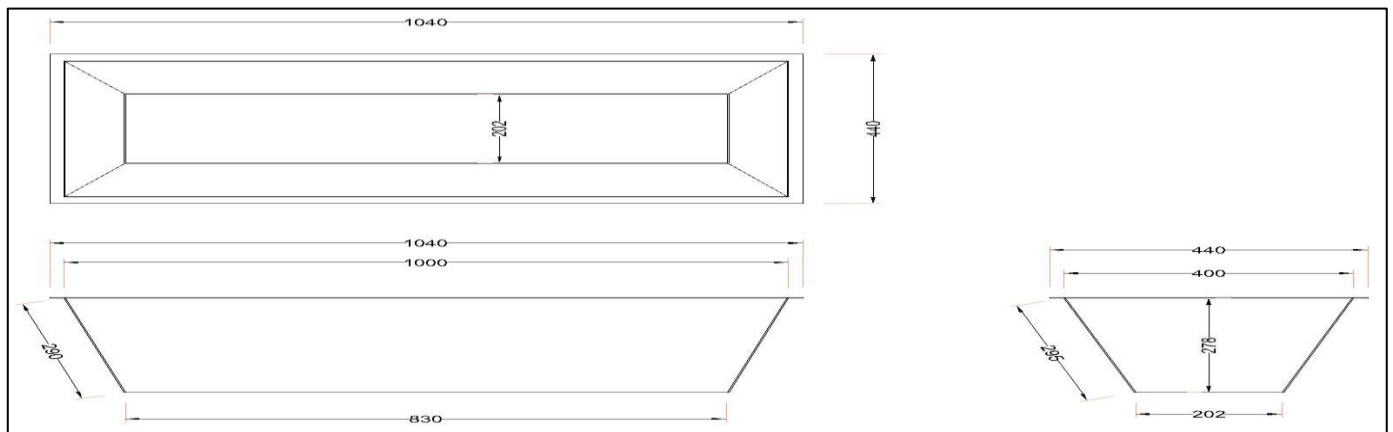


Fig 1: Feed Hopper of Cassava Peeling Machine

❖ *Slant Height of the Hopper*

The slant height is obtained from the relation in equation 9 (Akintunde, 2007)

$$H_s = \frac{H_h}{\cos \phi} \tag{9}$$

Where;

$H_s$  = Slant height, m

$H_h$  = Height of hopper = 0.278 m

$\phi$  = Angle of repose of cassava = 79.6°

$$H_s = \frac{0.278}{\cos 79.6} = 1.54 \text{ m}$$

❖ *Surface Area of Hopper Material*

The surface area of the hopper material is given by equation 10 (Ademosu, 2008)

$$A = \frac{1}{2} (a + b) \times h \tag{10}$$

The area of the hopper equates to the area of sheet 1 x 2 pieces and the area of sheet 2 x 2 pieces.

- Sheet 1 is sloped by 85 mm = 1000 mm – 830 mm = 170 mm ÷ 2 = 85 mm
- Sheet 2 is sloped by 101.5 mm = 400 mm – 202 mm = 198 mm ÷ 2 = 99 mm

Using Pythagoras' theorem to find the length of slopped sheet 1 and 2.

✓ *Sheet 1*

The vertical height = 278 mm

The slopped length = 85 mm

Pythagoras' theorem =  $a^2 + b^2 = c^2$

$$= \sqrt{a^2 + b^2}$$

$$= \sqrt{85^2 + 278^2}$$

$$= 291 \text{ mm}$$

✓ *Sheet 2*

The vertical height = 278 mm  
 The slopped length = 99 mm  
 Pythagoras' theorem =  $a^2 + b^2 = c^2$   
 $= \sqrt{a^2 + b^2}$   
 $= \sqrt{99^2 + 278^2}$   
 $= 295 \text{ mm}$

✓ *Area of Sheet 1*

Area of a trapezium =  $\frac{1}{2}(a + b) \times h$   
 $= 0.5(0.83 + 1) \times 0.291$   
 $= 0.266 \text{ m}^2$   
 We have 2 sides =  $0.266 \times 2 = 0.532 \text{ m}^2$

✓ *Area of Sheet 2*

Area of a trapezium =  $\frac{1}{2}(a + b) \times h$   
 $= 0.5(0.202 + 0.4) \times 0.295$   
 $= 0.089 \text{ m}^2$

We have 2 sides =  $0.089 \times 2 = 0.178 \text{ m}^2$

The total surface area of the hopper is  $0.532 + 0.178 = 0.71 \text{ m}^2$

❖ *Volume of Hopper Material,  $V_{hm}$*

The volume of hopper material was obtained by multiplying the hopper surface area by the thickness of material using equation 11.

$$V_{hm} = S_{ah} \times t \tag{11}$$

Where;

$t$  = Thickness of mild steel = 1.2 mm = 0.0012 m

$S_{ah}$  = Surface area of hopper = 0.71 m<sup>2</sup>

$V_{hm} = 0.71 \text{ m}^2 \times 0.0012 \text{ m} = 8.52 \times 10^{-4} \text{ m}^3$

$v$ . Weight of the hopper,  $W_h$

The weight of the hopper was determined from the density of the mild steel used in construction (7850kg/m<sup>3</sup>), surface area and thickness of the material. The mass of the hopper was determine by equation 12;

$$W_h = \rho H_{sa} t = \rho V_{hm} \tag{12}$$

Where  $H_{sa}$  = surface area of hopper = 0.71 m<sup>2</sup>

$\rho$  = density of mild steel = 7850 kg/ m<sup>3</sup>

$W_h = 7850 \times 8.52 \times 10^{-4} \text{ m}^3 = 6.6882$

$W_h = 6.6882 \text{ kg} = 65.588 \text{ N}$

➤ *Belt Drive Design*

Belts are used to transmit power from one shaft to another by means of pulleys, which rotate at the same speed or at different speeds. The procedure for selecting a V-belt drive is dependent on the motor horse power and the speed (rpm) rating. V-belts are rated from class A to E (Khurmi and Gupta, 2013).

❖ *Velocity of Drum Pulley*

The diameter of the pulley (D) may be obtained either from velocity ratio consideration or centrifugal stress consideration. The centrifugal stress induced in the rim of the pulley where determined using equation 13:

$$\sigma_t = \rho.v^2 \tag{13}$$

$\rho$  = Density of the rim material

= 7200 kg/m<sup>3</sup> for cast iron

$v$  = Velocity of the rim =  $\pi DN/60$ ,  $D$  being the diameter of pulley and  $N$  is speed of the pulley

Equation 13 is applied to both flat and V-belts.

From a similar design by Olaoye *et al.* (2011), the value of  $\sigma_t$  = 4.5 MPa =  $4.5 \times 10^6 \text{ N/m}^2$  as centrifugal stress for v-belt

$$\sigma_t = \rho.v^2$$

$$4.5 \times 10^6 = 7200 \text{ kg} \times V^2$$

$$\frac{4.5 \times 10^6}{7200} = V^2$$

$$V^2 = \frac{4.5 \times 10^6}{7200}$$

$$V^2 = 625$$

$$V = \sqrt{625}$$

$$V = 25 \text{ m/s}$$

❖ *Diameter of the Electric Motor Pulley*

$$V = \frac{\pi DN}{60} \tag{14}$$

$N$  = Speed of motor = 1400 rpm

$$25 = \frac{3.142 \times D \times 1400}{60}$$

$$1500 = 4398.8$$

$$D = \frac{1500}{4398.8}$$

$$D = 0.3410 \text{ m}$$

$$D = 34.10 \text{ mm}$$

From Khurmi and Gupta, the diameter of pulleys in mm for flat and V-belts has 34.10mm between 32mm and 36mm; hence we shall select a 36mm diameter pulley.

❖ *Determination of the Diameter of Drum Pulley*

The speed of the drum pulley from equation 15;

$$v.r = \frac{N_2}{N_1} = \frac{d_1}{d_2} \tag{15}$$

$N_1$  = Speed of the electric motor pulley

$N_2$  = Speed of the drum pulley

$d_1$  = Diameter of the electric motor pulley

$d_2$  = Diameter of the drum pulley

A velocity ratio of 0.288 is adopted as reported from Olunkule and Akinnuli (2013).

$$d_1 = 36 \text{ mm}$$

$$N_1 = 1400 \text{ rpm}$$

$$0.288 = 36/d_2$$

$$d_2 = 36/0.288$$

$$d_2 = 125 \text{ mm}$$

Hence,  $N_2 = 403.2 \text{ rpm}$   
 Say; 405 rpm

According to Khurmi and Gupta (2013), the distance between two pulleys is twice the diameter of the larger pulley.

$$X = 2d_2$$

Where;

X = distance between the two pulleys.

$$X = 2 \times 125 \text{ mm}$$

$$X = 250 \text{ mm}$$

✓ *Belt length*

The belt length  $L_1$  was determined using equation 16 (Khurmi and Gupta 2013).

$$L = 2X + \frac{\pi}{2}(d_1 + d_2) + \frac{(d_2 - d_1)^2}{4X} \quad (16)$$

Where;

$x_c$  = Distance between pulley centers, mm

$d_1$  = Driver (motor) pulley diameter, mm

$d_2$  = Driven pulley diameter, mm

✓ *Belt Length from Motor to Drum*

$d_1 = 36 \text{ mm}$ ,  $d_2 = 125 \text{ mm}$  and  $X = 250 \text{ mm}$

$$L = 2 \times 250 + \frac{\pi}{2}(36 + 125) + \frac{(125 - 36)^2}{4 \times 250}$$

$$L = 761.212 \text{ mm}$$

✓ *Belt Contact or Rap Angle*

Bhandari, (1994) stated the contact angle of an open belt drive is as follows;

$$\text{For big pulley: } \theta_1 = 180^\circ + 2\sin^{-1}\left(\frac{r_2 - r_1}{X}\right) \text{ degree} \quad (17)$$

Where;

$r_2$  = Radius of big pulley,

$r_1$  = Radius of small pulley,

X = Distance between pulley centers.

$$\text{The angle in radians } \theta_1 = \theta_1^\circ \times \frac{\pi}{180^\circ}$$

$$\text{For small pulley: } \theta_1 = 180^\circ - 2\sin^{-1}\left(\frac{d_2 - d_1}{X}\right) \text{ degrees} \quad (18)$$

The smaller pulley governs the design.

❖ *Distance between Motor Pulley and Drum Pulley (For small pulley)*

Substituting  $d_2 = 125 \text{ mm}$ ,  $d_1 = 36 \text{ mm}$ ,  $X = 250$

$$\theta_1 = 180^\circ - 2\sin^{-1}\frac{62.5 - 18}{250} = 159.493^\circ$$

The angle in radians;

$$\theta_1 = 163.03 \times \frac{\pi}{180^\circ} = 2.78 \text{ radians}$$

❖ *Belt Tension from Motor to Drum*

V-belt: According to Khurmi and Gupta, (2013) V-belt is mostly used where a great amount of power is to be transmitted, from one pulley to another, when the two pulleys are very near to each other. Where both pulleys rotate in the same direction open belt drive is used. Therefore, V-belt was used.

Class B V-belt was chosen for the design. Leather material with belt density of  $1000 \text{ kg/m}^3$  (Appendix 1.1) and coefficient of friction of 0.25 on dry cast iron was chosen (Appendix 1.2).

For type B belt, a groove angle  $2\beta$  of 32 was chosen (Appendix 1.3). According to IS: 2494 1974 the dimensions of standard v-belt were chosen (Appendix 1.4) (Khurmi and Gupta, 2013).

Power range	2 - 15 KW
Minimum pitch diameter of pulley (D)	125 mm
Top width (b)	17 mm
Thickness (t)	11 mm
Weight (w)	1.89 N/m

The power transmitted by a belt drive is a function of the belt tensions and belt speed.

It has been shown by experience that under average conditions an allowable stress of 2.8 MPa or less will give a reasonable belt life. An allowable stress ( $\sigma$ ) of 1.75 MPa (Nmm), width of 17mm and thickness of 11mm was chosen for the design (Khurmi and Gupta 2013).

The maximum tension was calculated using equation 19;

$$\sigma = \frac{T_1}{a} \quad (19)$$

Where;

$T_1$  = Maximum tension, N

a = Area of belt = b x t = 17 x 11 = 187 mm<sup>2</sup>

$\sigma$  = Allowable stress = 1.75 N/mm<sup>2</sup>

$$T_1 = 187 \times 1.75 = 327.25 \text{ N}$$

❖ *Ratio of Driving Tensions from Motor to Drum*

The tension caused by centrifugal force is called centrifugal tension. According to Khurmi and Gupta (2008), the effect of centrifugal tension is considered at higher belt speeds of more than 10m/s in the design. The maximum tension in the belt was obtained from equation 20 given by Khurmi and Gupta (2008).

$$T = \sigma a \tag{20}$$

Where;

- T = maximum tension (N),
- $\sigma$  = allowable stress (Mpa),
- a = area of belt (mm<sup>2</sup>),
- b = width of belt = 17 mm,
- t = thickness of belt = 11 mm.
- $T = \sigma bt = 1.75 \times 17 \times 11 = 327.25$  N

The centrifugal tension will not be considered for the design; therefore the tension in the tight side of the belt (T<sub>1</sub>) will be equal to the maximum tension (T).

$$2.3 \text{ Log} \left( \frac{327.25}{T_2} \right) = \mu \theta \text{ cosec} \beta = 0.3 \times 2.78 \times \text{cosec} 16^\circ \frac{327.25}{T_2} = \text{Log}^{-1} \left( \frac{0.3 \times 2.78 \times \text{cosec} 16^\circ}{2.3} \right) = 20.54 \quad T_2 = \frac{327.25}{2.3835} = 15.93 \text{ N}$$

Total tension of the belt on the pulley = T<sub>1</sub>+T<sub>2</sub> = 327.25 + 15.93 = 343.18 N.

➤ *Design of Shaft*

A shaft is a rotating machine element used to transmit power from one place to another. The main shaft transmits power from the electric motor to the cylinder. Therefore, the shaft was designed based on strength and rigidity.

- *Shaft Diameter*

The machine has four (4) shafts. One shaft is developed into a rasped peeling drum. This one does superficial peeling. Another shaft is developed into a iron brush peeling drum. This one does deep peeling and peeling around irregularly shaped cassava roots. The remaining two (2) shafts are developed into a plastic brushes drum to clean the peeled cassava roots.

Since mild steel was used for the shaft, maximum shear stress theory was used for the design of the shaft diameter and it is given in equation 22 (Khurmi and Gupta 2008).

$$d^3 = \frac{16}{\pi S_s} \sqrt{(K_b M_b)^2 + (K_t M_t)^2} \tag{22}$$

Where;

- d = ?
- s = Maximum permissible shear stress (N/mm<sup>2</sup>),
- $S_s = \frac{\text{Ultimate Strength in Shear}}{\text{Factor of Safety, FS}}$  (23)
- K<sub>b</sub> = Combined shock and fatigue factor applied to bending moment,
- K<sub>t</sub> = Combined shock and fatigue factor applied to torsional moment,
- M<sub>b</sub> = Maximum bending moment, Nm,
- M<sub>t</sub> = Torsional moment, Nm.
- K<sub>b</sub> = 1.5 and K<sub>t</sub> = 1.0 for gradually applied or steady load. S<sub>s</sub> = 42 MPa for shaft with key way (Khurmi and Gupta 2013). Assuming a factor of safety (F.S) of 1.5, the maximum permissible shear stress for shaft with key way is;
- $S_s = \frac{42 \text{ MPa}}{F.S} = \frac{42 \text{ MPa}}{1.5} = 28 \text{ Mpa}$

$$T_1 = T = 327.25 \text{ N}$$

According to Khurmi and Gupta (2013), the included angle for V-belt is from 30° to 40° and the ratio of driving tensions is given by equation 21;

$$2.3 \text{ Log} \left( \frac{T_1}{T_2} \right) = \mu \theta \text{ cosec} \beta \tag{21}$$

Where;

- T<sub>1</sub> = Tension on the tight side (N),
- T<sub>2</sub> = Tension on loose side (N),
- $\mu$  = Coefficient of friction between belt and pulley = 0.3
- $\theta$  = Angle of contact = 2.78 radians,
- $\beta$  = Semi-groove angle of the pulley = 16°

- *Vertical Loading on Shafts*

$$d^3 = \frac{16}{\pi S_s} \sqrt{(K_t M_b)^2 + (K_t M_b)^2}$$

where d = ?

$$S_s = \frac{42 \text{ MPa}}{F.S} = \frac{42 \text{ MPa}}{1.5} = 28 \text{ Mpa}$$

To find M<sub>b</sub> and M<sub>t</sub>

For belt drive, according to Khurmi and Gupta (2013), the torque transmitted is given by equation 24;

$$M_t = (T_1 - T_2)R \tag{24}$$

Where;

- M<sub>t</sub>= Torsional moment, Nm,
- T<sub>1</sub> = Tension in tight side = 327.25 N,
- T<sub>2</sub> = Tension in loose side = 15.93 N,
- R = Radius of drum pulley = 62.5 mm = 0.0625 m
- M<sub>t</sub> = (327.25 – 15.93) x 0.0625 = 20.24 Nm

The shafts to be used in the machines shall be designed based on the recommendations from Ademosun *et al.* (2012). They selected a standard shaft of 0.6m length having a rasped-drum and self-weight of 2.0kg. They also recommended 10kg of cassava per batch for peeling. The vertical loading on the shaft is shown in figure 4.

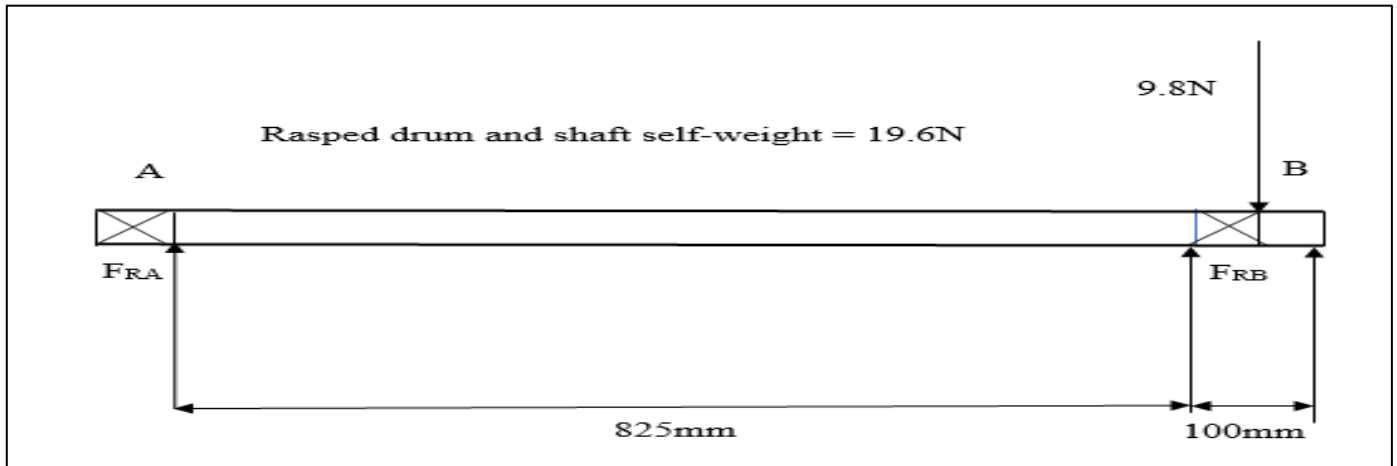


Fig 4: Bending Loads of the Shaft

➤ *To Determine the Bending Moments*

Taking moments about  $F_{RA}$ , we have;

$$\begin{aligned} F_{RB} \times 825 &= 9.8 \times 925 + 54.39 \times 462.5 \\ F_{RB} \times 825 &= 9065 + 25155.375 \\ F_{RB} \times 825 &= 34220.375 \\ F_{RB} &= 34220.375/825 \\ &= 41.479 \text{ N} = 41.50 \text{ N} \end{aligned}$$

And

$$\begin{aligned} F_{RA} &= (54.39 + 9.8) - 41.50 \\ &= 64.19 - 41.50 \\ &= 22.69 \text{ N} \end{aligned}$$

Bending Moment at A

$$= F_{RA} \times 462.5 = 22.69 \times 462.5 = 10494.125 \text{ N-mm} = 10.494 \times 10^3 \text{ N-mm}$$

And bending moment at B

$$= F_{RB} \times 100 = 41.50 \times 100 = 4150 \text{ N-mm} = 4.15 \times 10^3 \text{ N-mm}$$

The maximum bending moment is at A, therefore maximum bending moment,  $M_B = 10.494 \times 10^3 \text{ N-mm}$ .

• *Diameter of Shaft for Vertical Load on the Shaft is Calculated as;*

$$M_b = 10.494 \times 10^3 \text{ N-mm} = 10.494 \text{ N-m}$$

$$M_t = 20.24 \text{ N-m}$$

$$S_s = 28 \text{ Mpa}$$

$$d^3 = \frac{16}{\pi S_s} \sqrt{(K_b M_b)^2 + (K_t M_t)^2}$$

$$d^3 = \frac{16}{3.142 \times 28 \times 10^6} \sqrt{(1.5 \times 10.494)^2 + (1.0 \times 20.24)^2}$$

$$= 1.8187 \times 10^{-7} \sqrt{247.779081 + 409.6576}$$

$$= 1.8187 \times 10^{-7} \sqrt{657.436681}$$

$$= 1.8187 \times 10^{-7} \times 25.6405281$$

$$d^3 = 4.663242845 \times 10^{-6}$$

$$d = \sqrt[3]{3.812635509 \times 10^{-6}}$$

$$d = 0.0167069053 \text{ m}$$

$$d = 16.70 \text{ mm say, } 20 \text{ mm.}$$

• *Determination of Power Delivered by Pulley to Drive the Four (4) Shafts.*

The rated power of the shaft is the power supplied by pulley and is given by equation 25;

$$\begin{aligned} P &= (T_1 - T_2) V \tag{25} \\ &= (327.25 - 15.93) \times 25 \\ &= 7783 \text{ W} \\ &= 7.783 \text{ kW} \\ 1 \text{ hp} &= 745.69 \text{ w} \\ 7783 \text{ W} &= 10.43 \text{ hp} \end{aligned}$$

• *Torsional Deflection of the Shaft Connected to Pulley*

According to Khurmi and Gupta (2013), the permissible angle of twist should not exceed 0.25 degrees per meter length for machine tool shafts. For line shafts or transmission shafts, the permissible angle of twist should not exceed 3 degrees per meter length. The angle of twist was determined from equation 26 (Khurmi and Gupta, 2013);

$$\theta = \frac{584 M_t L}{G d^4} \quad (\text{For solid shaft}) \tag{26}$$

Where;

$\theta$  = Angle of twist, deg,

L = Length of shaft = 0.6 m,

$M_t$  = Torsional moment = 20.24 Nm

G = Torsional modulus of elasticity = 80 GN/m<sup>2</sup>,

d = Shaft diameter = 0.020 m

$$\theta = \frac{584 \times 20.24 \times 0.6}{80 \times 10^9 \times 0.020^4} = 0.55407 = 0.55^\circ$$

Since the angle of twist (0.55 degree/m) calculated is less than the maximum permissible angle of twist (3 deg/m) for line shafting, the shaft design is safe (Khurmi and Gupta, 2013).

➤ *Design of Chain and Sprocket*

• *The Velocity Ratio of the Chain*

Ademosun *et al.* (2012) recommended a velocity ratio of 3 for a chain and sprocket system in drawing power from a belt and pulley drive of velocity ratio of 0.288. The velocity ratio was determined using equation 27 (Khurmi, 2006)

$$\text{Velocity ratio (V.R)} = \frac{N_1}{N_2} = \frac{T_2}{T_1} \tag{27}$$

Where,

$N_1$  = speed of the small sprocket

$N_2$  = speed of the big sprocket

$T_1$  = number of teeth of the small sprocket

$T_2$  = number of teeth of the big sprocket

• *Number of Teeth on the Smaller Sprocket*

From appendix 2.4 the number of teeth for a smaller sprocket at velocity ratio of 3 and roller chain type are 25.

• *Number of Teeth on the Bigger Sprocket*

The number of teeth on the bigger sprocket using equation 28 (Khurmi, 2006)

$$\begin{aligned} T_2 &= T_1 \times 3 \\ T_2 &= 25 \times 3 \\ &= 75 \end{aligned} \tag{28}$$

Number of  $T_1 = 25$

$T_2 = 75$

• *Determination of Chain Parameter*

According to Indian Standards (IS: 2403 —1991), the various characteristics for 8B type chain (Khurmi, 2005) are:

Pitch (P) = 12.70 mm

Roller diameter  $d_1 = 8.51$  mm

Minimum width of roller ( $b_1$ ) = 7.75

Transverse pitch ( $P_1$ ) mm = 13.92 mm

Breaking load (KN) minimum = 17.8 kN

• *Pitch Circle Diameter and Pitch Line Velocity of the Smaller Sprocket*

The pitch circle diameter and pitch line velocity of the smaller sprocket can be determined using equation 29 and 30 respectively

Pitch circle diameter ( $d_1$ )

$$d_1 = P \operatorname{cosec} \left( \frac{180}{T_1} \right) \tag{29}$$

P = pitch (mm) = 12.7 mm = 0.0127 m

$T_1$  = number of teeth on smaller sprocket = 25

$$\begin{aligned} d_1 &= 0.0127 \operatorname{cosec} \left( \frac{180}{25} \right) \\ &= 0.0127 \times 7.98 = 0.101 \text{ m} = 101 \text{ mm} \end{aligned}$$

$$d_2 = P \operatorname{cosec} \left( \frac{180}{T_2} \right) \tag{30}$$

$$= 0.0127 \times 22.29 = 0.283 \text{ m} = 283 \text{ mm}$$

• *Pitch Line Velocity*

$$V_1 = \frac{\pi d_1 N_1}{60} \tag{31}$$

$N_1$  = r.p.m of smaller sprocket = 1215 rpm

$$V_1 = \frac{3.142 \times 0.101 \times 500}{60} = 6.43 \text{ m/s}$$

$$\begin{aligned} V_2 &= \frac{\pi d_2 N_2}{60} \\ &= \frac{3.142 \times 0.283 \times 405}{60} = 6.00 \text{ m/s} \end{aligned}$$

• *To Calculate Distance Between Sprocket*

According Khurmi and Gupta (2013), the minimum center distance between the smaller and larger sprocket should be 30 to 50 times the pitch. Taking it as 30 times the pitch.

$$\text{Center distance between sprockets} = 30 P = 30 \times 12.7 = 381 \text{ mm}$$

In other to accommodate initial sag in the chain, the value of centre distance is reduced by 2 to 5 mm.

$$\text{Correct centre distance (x)} = 381 - 4 = 377 \text{ mm}$$

The number of chain links (K) is

$$K = \frac{T_1 + T_2}{2} + \frac{2X}{p} + \left( \frac{T_2 - T_1}{2\pi} \right)^2 \frac{P}{X} \tag{32}$$

$$K = \frac{25 + 75}{2} + \frac{2 \times 377}{12.7} + \left( \frac{75 - 25}{2 \times 3.142} \right)^2 \frac{12.7}{377} = 0.03369$$

$$= 50 + 59.37 + 2.13 = 111.5$$

Say 112

• *Length of Chain*

$$L = K.P = 112 \times 12.7 = 1422.4 \text{ mm} = 1.42 \text{ m}$$

• *Power to Run Chain and Sprocket or Power Transmitted by Chain*

The power to drive the chain on the basis of breaking load is given by equation 33 (Khurmi and Gupta, 2008)

$$P_{CS} = \frac{W_B \times v}{n \times K_S} \tag{33}$$

$$\text{Safety factor (n)} = \frac{W_B}{W}$$

$$W = \frac{\text{rated power}}{\text{pitch line velocity}}$$

$W_b$  = breaking load in Newton's = 17.8 kN (appendix 2.5)

V = velocity of chain in m/s = 6.43 m/s

n = factor of safety

$K_S$  = service factor =  $K_1, K_2, K_3$

$K_1 = 1.23$  (For variable load with mild shock)

$K_2 = 1$  lubrication factor (for drop lubrication)

$K_3 = 1.25$  rating factor (for 16 hours per day)

$$K_S = 1.5 \times 1 \times 1.25 = 1.875$$

W = weight on chain

$$W = \frac{\text{rated power}}{\text{pitch line velocity}} = \frac{7.783}{6.43} = 1.210 \text{ KN} = 1210 \text{ N}$$

$$n = \frac{17.8 \times 10^3}{1210} = 14.71$$

$$P = \frac{17.8 \times 10^3 \times 6.43}{14.71 \times 1.875} = 4149.70 \text{ w} = 4.1497 \text{ kW}$$

From appendix 2.5 the breaking strength of the chain may be obtained by the following empirical relations.

➤ *Design of Drum*

The design was such that the hopper is vertically above the drum, the hopper empties its content into the drum which houses the rotary brushes that execute the peeling of the cassava.

The peeling drum was made of a cylinder of length 835 mm, thickness 2 mm and diameter 140 mm as recommended by Nwachukwu and Simonyan (2015)

• *Weight of Drum*

According to Hanna and Hillier (1999). The weight and volume of a cylinder drum are given by equation 34 and 35.

$$W_c = \rho_c V_c g \tag{34}$$

$$V_c = \pi D_c L_c t_c \tag{35}$$

$\rho_c$  = density of cylinder material = 7850 kg/m<sup>3</sup>

$V_c$  = volume of cylinder, m<sup>3</sup>

$g$  = acceleration due to gravit = 9.81 m/s<sup>2</sup>

$D_c$  = diameter of cylinder = 140 mm = 0.14 m

$L_c$  = length of cylinder = 835 mm = 0.835 m

$t_c$  = thickness of the cylinder = 2 mm = 0.002 m

Therefore,

$$V_c = 3.142 \times 0.14 \times 0.835 \times 0.002 = 7.35 \times 10^{-4} \text{m}^3$$

$$W_c = 7850 \times 7.35 \times 10^{-4} \times 9.81 = 56.60 \text{ N}$$

➤ *Brush Selection*

• *Wire Brushes*

The common wire brushes were welded on a shaft to form a cylindrical drum around a shaft to form a peeling drum. Iron brush was chosen because it will withstand the tangential force of the peeling drum and it will provide the shear strength to cause peeling. The mild steel shaft on which these brushes were mounted are 2 with a length of 0.6 m.

• *Synthetic Brushes*

The brush holder was made of melina wood and this made up the abrasive drum of the machine in which the synthetic brush is attached as shown in plate 5.



Plate 5: Brush Arrangement

➤ *Design for Shaft Bearings*

Bearings are used to prevent friction and subsequent wear of a rotating shaft. Almost every rotating member rotates on bearings. It is therefore important to select a bearing that will last for the predicted life during the course of operation. In the selection;

- A design life, L is selected in revolutions or hours
- Equivalent radial load, expected life, dynamic capacity and bearing life

✓ *Load on Bearing*

From the bending Loads of the Shaft (Figure 4), the reaction at A and B in vertical loading direction were calculated as  $R_A = 22.69 \text{ N}$  and  $R_B = 41.50 \text{ N}$ .

Since the drive was not inclined, the reaction at  $F_{RA}$  and  $F_{RB}$  in horizontal loading direction are equal to zero. From Figure 4, the load carried by bearing at point (A) has resultant and it will be determined using equation 36 (Hannah and Hillier, 1999).

$$F_{RA} = \sqrt{R_{AV}^2 + R_{AH}^2} \tag{36}$$

Where;

$R_{AV}$  = Reaction at A in vertical loading direction (N), = 22.69 N

$R_{AH}$  = Reaction at A in horizontal loading direction (N). = 41.50 N

The load carried by bearing at point (B) has resultant, it will be determined using equation 37 (Hannah and Hillier, 1999).

$$F_{RB} = \sqrt{R_{bV}^2 + R_{bH}^2} \quad (37)$$

Where;

$R_{bV}$  = Reaction at A in vertical loading direction (N),

$R_{bH}$  = Reaction at A in horizontal loading direction (N).

$$F_{ra} = \sqrt{22.69^2} = 22.69 \text{ N}$$

$$F_{rb} = \sqrt{41.50^2} = 41.50 \text{ N}$$

Since  $F_{ra}$  is greater than  $F_{rb}$ ,  $F_{ra}$  is now the criterion.

#### ✓ Equivalent Load

Equivalent load, P is given by equation 38 (Bhandari, 1994);

$$P = K_s(XVF_R + YF_A) \quad (38)$$

Where;

$F_R$  = Radial load (N),

$F_A$  = Thrust load (N),

X = Radial factor,

Y = Thrust factor,

$K_s$  = Service factor for moderate shock load,

V = Rotational factor for all types of bearings when the inner face is rotating.

$F_A = 0$  since there is no axial load. The values  $K_s = 2$ ,  $V = 1$ ,  $X = 1$ ,  $Y = 1$  (Bhandari, 1994).

Equivalent load becomes;

$$P = 2F_R \quad (39)$$

Where;

$F_R$  = Radial load = Load on bearings = 22.69 N

$$P = 2 \times 22.69 = 45.38 \text{ N}$$

#### ✓ Expected Life

The approximate rating (service) life of bearing is based on the fundamental equation 40 (Khurmi and Gupta, 2008).

$$L = \left(\frac{C}{P}\right)^k \times 10^6 \text{ revolutions} \quad (40)$$

Where;

L = Rated life (revolutions),

P = Equivalent load (N),

C = Basic dynamic load rating (N),

K = constant = 3 for ball bearings.

The relationship between the life in revolutions (L) and the life in working hours ( $L_H$ ) is given by Bhandari, (1994) in equation 41.

$$L = 60N.L_H \text{ revolutions} \quad (41)$$

Where;

N = Speed in rpm.

The highest speed in the system is at 1400rpm.

A recommended life of 4,000 hours to 8,000 hours for machines used for short periods or intermittently and whose breakdown would not have serious consequences e.g. hand

tools, lifting tackle in workshops, operated machines, agricultural machines, cranes in erecting shops and domestic machines was stated by Khurmi and Gupta (2008). It is assumed that the peeler falls in this category and has a rated life of 8,000 hours.

$$L = 60N.L_H$$

$$L = 60 \times 1400 \times 8000$$

$$L = 672 \times 10^6 \text{ revolutions}$$

#### ✓ Dynamic Capacity

The dynamic capacity, C was calculated from equation 42 (Bhandari, 1994).

$$C = P \left(\frac{L}{10^6}\right)^{1/k} \quad (42)$$

Where;

L = Rated life =  $672 \times 10^6$  revolutions,

P = Equivalent load = 45.38 N,

K = constant = 3 for ball bearings.

$$C = 45.38 \left(\frac{672 \times 10^6}{10^6}\right)^{1/3} = 397.4765 \text{ N}$$

$$C = \frac{397.4765}{9.81} = 40.52 \text{ kg}$$

#### ✓ Weight of Bearing

$$W_b = M_b g$$

$$m_b = \rho_b V_b$$

where,

$W_b$  = weight of bearing

$M_b$  = mass of bearing

g = acceleration due to gravity = 9.81 m/s<sup>2</sup>

$m_b = ?$

$\rho_b$  = density of mild steel = 7850 kg/m<sup>3</sup>

$V_b$  = volume of bearing =  $\pi r^2 h$

r = 0.03 m

h = 0.04

$$V_b = 3.142 \times 0.03^2 \times 0.04 = 1.13 \times 10^{-4}$$

$$m_b = 7850 \times 1.13 \times 10^{-4} = 0.887 \text{ kg}$$

$$w_b = 8.69 \text{ N}$$

$$\text{total weight of bearings} = 8.69 \times 8 = 69.52 \text{ N}$$

#### ✓ Bearing Life in Years

If the machine works for 8 hours per day, we have 365 days in a year which is 52 weeks in a year, excluding 52 Sundays in a year, the machine will work for;

$$365 \text{ days} - 52 \text{ days} = 313 \text{ days}$$

Assuming there are 20 days for public holidays;

$$313 \text{ days} - 20 \text{ days} = 293 \text{ days to work}$$

The assumed life in hours,

$$L_H = 8,000 \text{ hours.}$$

$$293 \text{ days} \times 8 \text{ hours} = 2344 \text{ hours}$$

Therefore, the bearing is supposed to last for;

$$\frac{8,000}{2344} = 3.4 \text{ years}$$

From the table of basic static and dynamic capacities of various types of radial ball bearings (Khurmi and Gupta, 2008), the bearing number 206 was selected. The bearing type is single row, deep groove, ball bearing and has the following parameters; bore (30 mm), width (16 mm) and outside diameter (62 mm).

✓ *Discharge Chute*

The discharge chute (figure 5) is the outlet for cassava chaff.

▪ *Surface Area of Discharge Chute*

The height of the rectangular section is assumed to be the same with the height of the trapezoidal section of the discharge chute. The value of the length and breadth for the rectangular section and the value of the height and breadth for the trapezoidal section were chosen so that the machine will not be extremely large. The surface area of the chute was determined using equation (43). The discharge chute is made up of rectangular section and trapezoidal section as shown in figure 5.

▪ *Surface area of the rectangular section*

$$S_{ar} = 2(l_d \times b_d) \tag{43}$$

Where;

$S_{ar}$  = Surface area of the rectangular section

$b_d$  = Length of the rectangular section = 0.141 m

$l_d$  = breadth of the rectangular section = 0.825 m

$$S_{ar} = 2(0.141 \times 0.825) = 0.233 \text{ m}^2$$

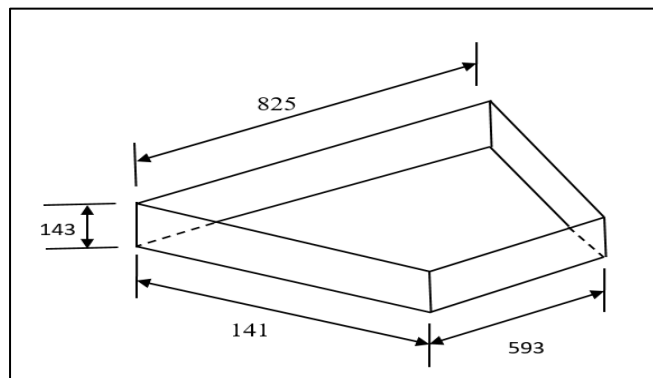


Fig 5: Discharge Chute

➤ *Surface Area of the Trapezoidal Section*

$$S_{at} = \frac{1}{2}(B_{tt} + B_{bt})h_{td} \tag{44}$$

Where;

$S_{at}$  = **Surface area of the trapezoidal section, m<sup>2</sup>**

$h_{td}$  = Height of trapezium = 0.143 m

$B_{tt}$  = Breadth of the trapezium at the top frustum= 0.825 m

$B_{bt}$  =Breadth of the trapezium at the base frustum= 0.593 m

$$S_{at} = \frac{1}{2}(0.825 + 0.593)0.143 = 0.101 \text{ m}^2$$

• *Surface Area of Discharge Chute*

$$S_{ad} = S_{ar} + S_{at} \tag{45}$$

Where;

$S_{ad}$ = Surface area of discharge chute, m<sup>2</sup>

$S_{ar}$  = Surface area of rectangular section, m<sup>2</sup> = 0.233 m<sup>2</sup>

$S_{at}$  = Surface area of trapezoidal section, m<sup>2</sup> = 0.101 m<sup>2</sup>

$$S_{ad} = 0.233 + 0.101 = 0.334 \text{ m}^2$$

• *Volume of Discharge Chute, V<sub>dc</sub>*

The volume of discharge chute was obtained by multiplying the discharge surface area by the thickness of material as shown by equation 46.

$$V_{dc} = S_{ad} \times t \tag{46}$$

Where;

$t$  = Thickness of mild steel = 0.0012 m

$S_{ad}$ = Surface area of discharge = 0.334m<sup>2</sup>

$$V_{dc} = 0.334 \times 0.0012 = 0.0004008 \text{ m}^3 = 4.01 \times 10^{-4} \text{ m}^3$$

• *Mass of the Discharge Chute, M<sub>dc</sub>*

The mass of the discharge chute was determined from the density of the mild steel used in construction (7850kg/m<sup>3</sup>) and its volume. The mass of the discharge chute was determined by equation 47;

$$M_{dc} = \rho V_m \tag{47}$$

Where;

$M_{dc}$ = Mass of the discharge chute, kg

$M_{dt}$  = Total mass of the discharge chutes

$\rho$  = Density of mild steel = 7850 kg/m<sup>3</sup>

$V_m$  = Volume of discharge chute =  $4.01 \times 10^{-4} \text{ m}^3$

$$M_{dc} = 7850 \times 4.01 \times 10^{-4} = 3.15 \text{ kg}$$

$$W_{dc} = 3.15 \times 9.81 = 30.90 \text{ N}$$

➤ *Design of the Frame*

Rigidity and strength are the most important criteria considered for the frame design. The frame design involves knowing the kind of load that it will be subjected to, selecting the correct steel sections for the frame construction and analyzing all possible forms of failure that could occur on the frame to ensure safety of the design as shown in fig 6. The envisaged main-frame will be made of mild steel material.

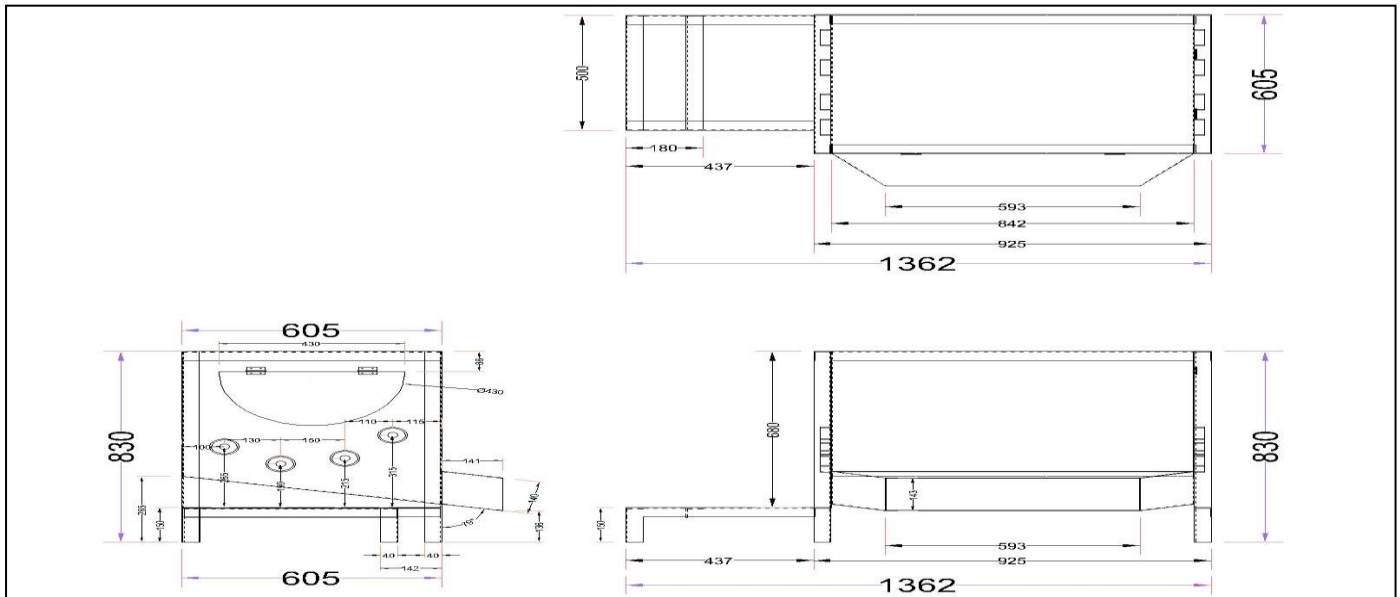


Fig 6: Machine Frame

• *Size of Frame*

The total weight acting on the frame is the weight of the peeling drum and the electric motor. The weight aggregate includes the weight of the hopper, delivery chute, peeling drum, flywheel, pulleys, casings and mechanical engine. It is assumed that:

- The frame is fixed,
- The total load acting on the frame is uniformly distributed,
- The frame was constructed with a 40 × 40 angle iron of 3 mm thickness.

The frame was designed based on Euler’s column assumption (Khurmi and Gupta, 2008) which are:

- The cross-section of the column was uniform throughout its length,
- The column material is perfectly elastic, homogeneous and isotropic, and thus obeys Hooke’s law,
- The length of the column is very large as compared to its cross-sectional dimensions,
- The shortening of column, due to direct compression, which is very small is neglected,
- The failure of column occurs due to buckling alone,
- The weight of the column itself is neglected.

A standard angle iron of the following dimension was used.

Width = a = 40 mm  
Thickness = t = 3 mm

The angle iron was designed based on the formula given by Ryder (1983) in equation 48;

• *Area of Section, A*

$$A = t(2a - t) \tag{48}$$

Where,

- A = Area of section (mm<sup>2</sup>),
  - a = Breadth of section = 40 mm,
  - t = Thickness of section = 3 mm.
- $$A = 3(2 \times 40 - 3) = 231 \text{ mm}^2$$

Distance from neutral axis to external fibre, y using the equation 49;

$$y = a - \frac{a^2 + at - t^2}{2(2a - t)} \tag{49}$$

$$y = 40 - \frac{40^2 + 40 \times 3 - 3^2}{2(2 \times 40 - 3)} = 28.89 \text{ mm}$$

• *Moment of Inertia, I*

$$I = \frac{1}{3} [ty^3 + a(a - y)^3 - (a - t)(a - y - t)^3] \tag{50}$$

$$I = \frac{1}{3} [3 \times 28.89^3 + 40(40 - 28.89)^3 - (40 - 3)(40 - 28.89 - 3)^3]$$

$$I = 35818.19 \text{ mm}^4$$

• *Section modulus, Z*

Section modulus, Z was calculated from the equation 51;

$$Z = \frac{I}{y} \tag{51}$$

$$Z = \frac{35818.19}{28.89} = 1239.81 \text{ mm}^3$$

• *Radius of Gyration, K*

Radius of gyration, K was calculated using the equation 52;

$$K = \sqrt{\frac{I}{A}} \tag{52}$$

$$K = \sqrt{\frac{35818.19}{231}} = 12.45 \text{ mm}$$

According to Euler’s theory, the crippling or buckling load ( $W_{cr}$ ) under both end fixed conditions is represented by a general equation given by Khurmi and Gupta, (2008) as

$$W_{cr} = \frac{C\pi^2EI}{L^2} = \frac{C\pi^2EAK^2}{L^2} \quad (53)$$

Where;

- $W_{cr}$  = Crippling or buckling load, N
- C = Constant, representing the end conditions of the column or end fixity coefficient = 4 (both end fixed) (Khurmi and Gupta, 2008),
- E = Modulus of elasticity or young’s modulus for the material of the column =  $2 \times 10^5 \text{ N/mm}^2$ ,
- I =  $AK^2$  = Moment of inertia =  $35818.19 \text{ mm}^4$ ,
- A = Area of cross-section =  $231 \text{ mm}^2$ ,
- K = Least radius of gyration of the cross-section = 12.45 mm,
- L = Length of the column = 1023 mm.

$$W_{cr} = \frac{4 \times \pi^2 \times 200000 \times 35818.19}{1362^2} = 152454.1157 \text{ N} = 15545.99335 \text{ kg}$$

• *Total Weight on Frame*

- Weight of hopper = 665.88 N
- Weight of discharge chute = 30.90 N
- Weight of shafts and peeling drums (4) =  $4 \times 56.60 \text{ N} = 226.4 \text{ N}$
- Weight of cassava = 98 N

Weight of bearings = 69.52 N

Therefore, total weight on the frame = 1090.7 N = 111.22 kg  
The designed load that will cause buckling is 15545.99335 kg. But since the load acting on the frame is 111.22 kg, it then means that the frame dimensions chosen can support the various machine components on it.

*F. Description of the Machine*

Figure 7 is the isometric drawing of the cassava peeling machine and figure 8 shows the exploded drawing of the cassava peeling machine. The orthographic drawing of the machine is shown in figure 9 while plate 6 is the photograph of cassava peeling machine. The machine comprises of hopper, peeling chamber, driving mechanism and discharge chute. The peeling chamber is made of thick brushes fixed on hollow drum attached to the shaft. The shaft is supported by bearings at its ends and powered by electric motor via a belt and pulley drive arrangement that runs at desired speed and the speed is transmitted to other shafts via chain and sprocket arrangement. The discharge tray is made of steel metal tilted at a designed angle. The Machine is a batch type peeler, where the cassava tubers is fed into the system between four concentric circular peeler drums with brush materials attached round inside the perimeter of the drum. The circular drums peelers move in rotary motion which in turn peels the cassava as it moves. During peeling, water is added for washing and cleaning the tubers as well as to discharge the peeled wastes. In operation, the cassava was introduced into the peeling chamber via hopper and the machine peels the cassava. The peeled cassava is discharged through the discharge unit and was collected in a trough underneath. The machine is powered by an electric motor.

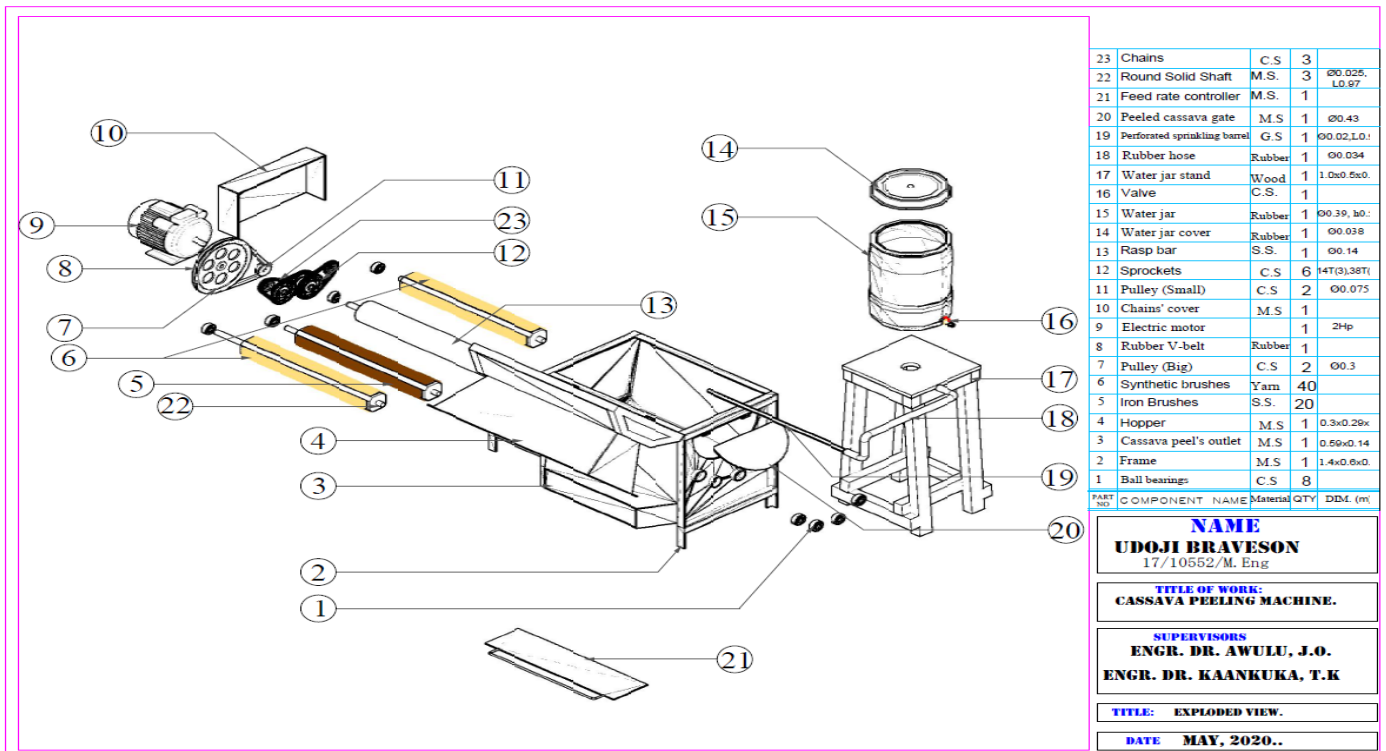


Fig 8: Exploded View of Cassava Peeling Machine

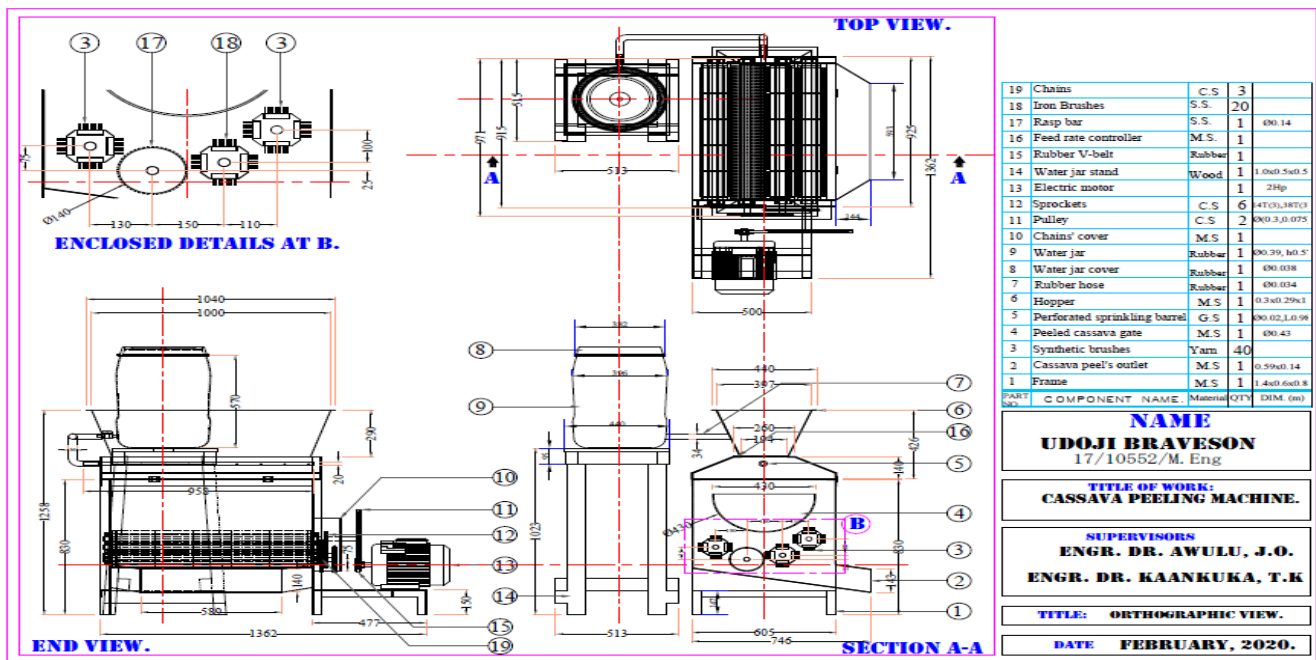


Fig 8: Orthographic Drawing of Cassava Peeling Machine



Plate 6: The Cassava Peeling Machine

**G. Performance Evaluation of the Machine**

➤ **Throughput Capacity**

Throughput capacity, T<sub>c</sub> (kg/h) was determined using equation 54 given by Nathan *et al* (2017).

$$T_c = \frac{M_t}{T} \quad (54)$$

Where;

T<sub>c</sub> = Throughput capacity (kg/h)

M<sub>t</sub> = mass of the cassava tuber fed into the machine (kg)

T = Time taken for cassava and its peels (peeling) to completely leave the machine (h)

➤ **Peeling Efficiency**

The peeling efficiency of the machine was determined using equation 55 as given by Oluwole and Adio (2013).

$$\eta_p = \frac{M_m}{M_T} \times 100 \% \quad (55)$$

Where;

η<sub>p</sub> = peeling efficiency (%),

M<sub>m</sub> = Weight of peels removed by the machine (kg),

M<sub>T</sub> = Total weight of peels (kg).

➤ **Percentage flesh loss of tubers**

Percentage flesh loss of tubers was calculated using equation 56 given by Agrawal (1987).

$$F_L = \frac{M_f}{M_f + M_c} \times 100 \% \quad (56)$$

Where;

F<sub>L</sub> = Percentage flesh loss of tubers (%)

M<sub>f</sub> = Weight of tuber portion which was removed along with the peel by the machine (kg),

M<sub>c</sub> = Weight of completely peeled tuber (kg).

▪ *Percentage Peeling Loss*

The percentage material loss in peeling is a measure of the effectiveness of the peeling chamber and was determined using equation 57.

$$M_L = \frac{W_{BP} - W_{AP}}{W_{BP}} \times 100 \% \tag{57}$$

Where;

$M_L$  = Percentage material loss (%)

$W_{BP}$  = Cassava weight before peeling (kg)

$W_{AP}$  = Cassava weight after peeling (kg).

➤ *Percentage Weight of Peels*

The percentage weight of peels was calculated using equation 58 as given by Oluwole and Adio (2013).

$$P_w = \frac{W_p}{W_{up}} \times 100 \% \tag{58}$$

Where;

$W_p$  = weight of peels (kg)

$W_{up}$  = weight of unpeeled tubers (kg)

*H. Experimental Design and Statistical Analysis*

➤ *Design of Experiment*

I-optimal responses surface design was used to model and optimize the operational parameters of the developed cassava peeling machine.

➤ *Statistical Analysis*

Design expert software version 10 was used to model and optimize the operational parameters of the developed cassava peeling machine.

*I. Cost of Producing the Cassava Peeler*

The estimated cost of producing the cassava peeler is divided into materials and labour costs as shown in Table 4.

Table 4: Material Specification and Costing of the Cassava Peeler

COMPONENT	MATERIAL	QUANTITY	UNIT PRICE (₦)	AMOUNT (₦)
Hopper	2mm mild steel sheet	$\frac{1}{2}$ sheet	5000	2500
Hopper hanger	40x40x4mm Angle iron	$\frac{1}{2}$ length	1000	500
Drum	2mm mild steel sheet	1 sheet	5000	5000
Discharge chute	2mm mild steel sheet	$\frac{1}{4}$ length	5000	1250
Frame	40x40x4mm Angle iron	3	1000	3000
Pulley	Cast iron	3	5000	15,000
V-belt	Leather	3	500	1500
Electric motor		1	30,000	30,000
Ball bearing		6	300	1800
Shaft	Mild steel	3	1500	4500
Bolt and nut	Mild steel	12	100	1200
Chains		2	800	1600
Sprockets		4	500	2000
Brushes		45	200	9000
Water jar	Rubber	1	1500	1500
Paint		1 tin	1200	1200
Electrodes	Gauge 12	1 pack	1500	1500
Labour cost				20,000
Transport				5000
<b>Sub total</b>				<b>108,500</b>
Miscellaneous		(10% of material cost + labour cost)		10805
<b>Grand Total</b>				<b>119,305</b>

**III. RESULTS**

Table 5 show the mathematical model equation for the cassava peeling process. Table 6 shows the experimental results obtained using an I-Optimal experimental design, for the purpose of evaluating and optimizing operational parameters of the developed cassava peeling machine. Factors used for evaluation and optimization are time and speed with levels ranging from 4 to 8 minutes and 380 to 460 m/s respectively. Evaluation results obtained for operational parameters of the machine, range from 82 – 160 kg/h, 39 – 75%, 1 – 4, 25 – 61.71%, 16 – 56.67% for throughput capacity, peeling efficiency, tuber damage, peeling weight

proportion and percentage flesh loss respectively. Table 7 shows the modeling analysis of the operational parameters of the developed cassava machine. Five models types were considered and tested during the modeling of each operational parameter. These models are linear, 2FI (2 Factor Interaction), quadratic and cubic. Statistic parameters used to test these models before considering the model to be chosen are Sequential p-value, Lack of Fit p-value, Adjusted R-Square, Predicted R-Square. Quadratic models were chosen to be the best for all operational parameters tested. Table 8 shows the ANOVA of the modeling terms of the operational parameters of the developed cassava peeling machine. All models developed for each operational parameter were

significant at  $P < 0.05$ . Also all model terms used in all equations developed for the operational parameters to be optimized were found to be significant at  $p < 0.005$ . Table 9 shows the Statistical properties of the model equations used for optimization of operational properties of the developed cassava peeling machine. Model for throughput capacity had

values of 2.632, 137.812, 1.91, 394.837, 68.861, 0.994, 0.992, 0.97, 58.321, 85.497 and 90.195 for Std. Dev., Mean, C.V. %, PRESS, -2 Log Likelihood, R-Squared, Adj R-Squared, Pred R-Squared, Adeq Precision, BIC, AICc respectively.

Table 5: Mathematical Model Equations for the Cassava Peeling Process

Parameters	Mathematical Model Equation	Coefficient of Determination ( $R^2$ )	Correlation Coefficient (R)
Peeling Efficiency (%)	$E = 0.134 S + 0.441 T + 37.648$	0.984	0.992
Percentage Flesh Loss of Tubers (%)	$L = 0.031 S + 0.106 T - 3.027$	0.997	0.998

E = Peeling Efficiency (%), L = Percentage Flesh Loss of Tubers (%), S = Machine Speed (rpm), T = Peeling Time (minutes).

Table 6: I-Optimal Response Surface Experimental Design Results for Evaluation and Optimization of Operational Parameters of the Developed Peeling Machine

Run	Factor	Factor	Response	Response	Response	Response	Response
	Time	Speed	Throughput Capacity	Peeling efficiency	Tuber damaged	Peeling weight proportion	Percentage flesh loss
	minute	m/s	kg/hr	%		%	%
1	8	460	82.5	39.28	2	60.71	56.67
2	8	420	90	44.44	2	55.56	50
3	4	380	135	64.28	1	35.71	16.67
4	6	460	160	61.54	4	38.46	33.33
5	4	460	150	58.82	1	41.18	23.33
6	8	420	90	44.44	2	55.56	50
7	6	420	160	62.74	3	37.25	31.67
8	6	420	160	62.74	3	37.25	31.67
9	4	380	135	64.28	1	35.71	16.67
10	6	420	160	62.74	3	37.25	31.67
11	4	420	135	56.25	1	43.75	23.33
12	4	380	135	64.28	1	35.71	16.67
13	6	460	160	61.54	4	38.46	33.33
14	6	420	160	62.74	3	37.25	31.67
15	8	380	112.5	60	3	40	33.33
16	6	380	180	75	3	25	20

Table 7: Modeling Analysis of Operational Parameters of the Developed Cassava Peeling Machine

Modeling parameter	Model considered	Sequential p-value	Lack of Fit p-value	Adjusted R-Square	Predicted R-Square	Software Decision
Throughput Capacity	Linear	0.123558		0.163558	-0.083504	
	2FI	0.188827		0.2200184	-0.372583	
	Quadratic	$4.24 \times 10^{-11}$		0.9921156	0.9700561	<b>Suggested</b>
	Cubic	$3.1 \times 10^{-5}$		0.9992645	0.9730487	Aliased
Peeling efficiency	Linear	0.020972		0.3632921	0.1546426	
	2FI	0.157113		0.4202734	0.10815	
	Quadratic	$3.76 \times 10^{-19}$		0.9998563	0.9994967	<b>Suggested</b>
	Cubic	0.091959		0.9999011	0.9963753	Aliased
Tuber damaged	Linear	0.086286		0.2085087	-0.109686	
	2FI	0.429954		0.1877131	-0.697659	
	Quadratic	$9.48 \times 10^{-6}$		0.903558	0.5465173	<b>Suggested</b>
	Cubic	$4.53 \times 10^{-6}$		0.9944383	0.7961991	Aliased
Peeling weight proportion	Linear	0.020932		0.3634837	0.1550097	
	2FI	0.157563		0.4202297	0.1082546	
	Quadratic	$2.84 \times 10^{-19}$		0.9998641	0.9995172	<b>Suggested</b>
	Cubic	0.073976		0.9999114	0.9967539	Aliased
	Linear	$6.32 \times 10^{-7}$		0.8716514	0.8100535	

Percentage flesh loss	2FI	0.020234		0.912889	0.8737011	
	Quadratic	1.9 x 10 <sup>-9</sup>		0.9981171	0.9910432	<b>Suggested</b>
	Cubic	0.001819		0.999514	0.9821902	Aliased

Table 8: ANOVA of Modeling Terms of Operational Parameters of the Machine

Modeling parameter	Source	Sum of Squares	Df	Mean Square	F - Value	p-value Prob > F	Software decision
Throughput Capacity	Model	13116.628	5	2623.325	378.497	4.68E-11	Significant
	Time	3798.415	1	3798.415	548.041	4.58E-10	Significant
	Speed	267.757	1	267.757	38.632	9.94E-05	Significant
	Time X Speed	688.266	1	688.266	99.304	1.64E-06	Significant
	Time <sup>2</sup>	8134.072	1	8134.072	1173.596	1.06E-11	Significant
	Speed <sup>2</sup>	214.977	1	214.977	31.017	0.000237	Significant
	Residual	69.308	10	6.93			
	Lack of Fit	69.308	3	23.102			
	Pure Error	0	7	0			
	Cor Total	13185.9375	15				
Peeling efficiency	Model	1229.754	5	245.95	20874.592	9.46E-20	Significant
	Time	271.419	1	271.419	23036.18	3.79E-18	Significant
	Speed	337.833	1	337.833	28672.938	1.27E-18	Significant
	Time X Speed	72.964	1	72.964	6192.758	2.68E-15	Significant
	Time <sup>2</sup>	544.628	1	544.628	46224.257	1.16E-19	Significant
	Speed <sup>2</sup>	99.754	1	99.754	8466.435	5.63E-16	Significant
	Residual	0.117	10	0.011			
	Lack of Fit	0.117	3	0.039			
	Pure Error	0	7	0			
	Cor Total	1229.87229	15				
Tuber damaged	Model	16.076	4	4.019	32.493	4.9E-06	Significant
	Time	3.708	1	3.708	29.981	0.000193	Significant
	Speed	0.049	1	0.049	0.403	0.538	Significant
	Time <sup>2</sup>	10.584	1	10.584	85.571	1.6E-06	Significant
	Speed <sup>2</sup>	0.754	1	0.754	6.101	0.031	Significant
	Residual	1.36	11	0.123			
	Lack of Fit	1.36	4	0.34			
	Pure Error	0	7	0			
	Cor Total	17.437	15				
Peeling weight proportion	Model	1229.971	5	245.994	22074.603	7.16E-20	Significant
	Time	271.497	1	271.497	24363.181	2.86E-18	Significant
	Speed	337.92	1	337.92	30323.738	9.58E-19	Significant
	Time X Speed	72.76	1	72.76	6529.277	2.06E-15	Significant
	Time <sup>2</sup>	544.83	1	544.83	48890.993	8.80E-20	Significant
	Speed <sup>2</sup>	99.667	1	99.667	8943.82	4.28E-16	Significant
	Residual	0.111	10	0.011			
	Lack of Fit	0.11143772	3	0.037			
	Pure Error	0	7	0			
	Cor Total	1230.083	15				
Percentage flesh loss	Model	2249.902	5	449.98	1591.316	3.65E-14	Significant
	Time	1268.698	1	1268.698	4486.641	1.34E-14	Significant
	Speed	393.201	1	393.201	1390.523	4.58E-12	Significant
	Time X Speed	87.268	1	87.268	308.618	7.59E-09	Significant
	Time <sup>2</sup>	108.661	1	108.661	384.27	2.61E-09	Significant
	Speed <sup>2</sup>	78.123	1	78.123	276.275	1.30E-08	Significant
	Residual	2.827	10	0.282			
	Lack of Fit	2.827	3	0.942			
	Pure Error	0	7	0			
	Cor Total	2252.73	15				

Table 9: Statistical Properties of Modeled Operational Parameters

Parameter Modeled	Model Equation	Model Properties	Values
Throughput Capacity	Quadratic	Std. Dev.	2.6326592
		Mean	137.8125
		C.V. %	1.9103196
		PRESS	394.83778
		-2 Log Likelihood	68.861797
		R-Squared	0.9947437
		Adj R-Squared	0.9921156
		Pred R-Squared	0.9700561
		Adeq Precision	58.321711
		BIC	85.497329
		AICc	90.19513
Peeling Efficiency	Quadratic	Std. Dev.	0.1085463
		Mean	59.069375
		C.V. %	0.1837608
		PRESS	0.6189686
		-2 Log Likelihood	-33.172523
		R-Squared	0.9999042
		Adj R-Squared	0.9998563
		Pred R-Squared	0.9994967
		Adeq Precision	533.49163
		BIC	-16.536991
		AICc	-11.83919
Tuber damaged	Quadratic	Std. Dev.	0.351698
		Mean	2.3125
		C.V. %	15.208561
		PRESS	3.9306717
		-2 Log Likelihood	5.9714972
		R-Squared	0.9219724
		Adj R-Squared	0.8935987
		Pred R-Squared	0.7745851
		Adeq Precision	15.043227
		BIC	19.834441
		AICc	21.971497
Peeling weight proportion	Quadratic	Std. Dev.	0.1055641
		Mean	40.925625
		C.V. %	0.2579412
		PRESS	0.593857
		-2 Log Likelihood	-34.064017
		R-Squared	0.9999094
		Adj R-Squared	0.9998641
		Pred R-Squared	0.9995172
		Adeq Precision	548.55569
		BIC	-17.428484
		AICc	-12.730683
Percentage flesh loss	Quadratic	Std. Dev.	0.5317636
		Mean	31.250625
		C.V. %	1.7016094
		PRESS	20.177166
		-2 Log Likelihood	17.676173
		R-Squared	0.9987448
		Adj R-Squared	0.9981171
		Pred R-Squared	0.9910432
		Adeq Precision	122.24882
		BIC	34.311705
		AICc	39.009506

Peeling Efficiency model had values of 0.109, 59.069, 0.184, 0.619, -33.172, 1.000, 1.000, 0.999, 533.492, -16.537, -11.839 for Std. Dev., Mean, C.V. %, PRESS,-2 Log Likelihood, R-Squared, Adj R-Squared, Pred R-Squared, Adeq Precision, BIC, AICc respectively. Model for Tuber damaged had values of 0.352, 2.313, 15.209, 3.931, 5.971, 0.922, 0.894, 0.775, 15.043, 19.834, 21.971 for Std. Dev., Mean, C.V. %, PRESS,-2 Log Likelihood, R-Squared, Adj R-Squared, Pred R-Squared, Adeq Precision, BIC, AICc respectively. Peeling weight proportion model had values of 0.106, 40.926, 0.258, 0.594, -34.064, 1.000, 1.000, 1.000, 548.556, -17.428, -12.731 for Std. Dev., Mean, C.V. %, PRESS,-2 Log Likelihood, R-Squared, Adj R-Squared, Pred R-Squared, Adeq Precision, BIC, AICc respectively. Then for Percentage flesh loss model had values of 0.532, 31.251, 1.702, 20.177, 17.676, 0.999, 0.998, 0.991, 122.249, 34.312, 39.010 for Std. Dev., Mean, C.V. %, PRESS,-2 Log Likelihood, R-Squared, Adj R-Squared, Pred R-Squared, Adeq Precision, BIC, AICc respectively. Figure 10, 11, 12, 13, 14, display diagnostics graphs of the models for the operating parameter of the developed cassava peeling machine. All data points lies along the diagonal of the actual and the predicted graph, for all models diagnosed. Table 10 show the optimization constrain and solutions for operational parameters of the developed cassava peeling machine while

Table 11 show the confirmation report on the models of the operational parameters used for optimization. All experimental observed values lies between the 95% PI (predicted Interval) low and the 95% PI high for all operational parameters modeled to valid the models. To optimize Time, Speed, Throughput Capacity , Peeling efficiency, Tuber damage, Peeling weight proportion, percentage flesh loss a constrain (goal) of : in range, in range, in range, maximize, minimize, minimize, minimize were placed on the optimizing parameters respectively. The optimized solution ranges from 4 – 8 minutes, 380 – 460 m/s, 138 – 171 kg/h, 58 – 74 %, 1 – 4, 25 – 41 %, 16 – 28 % for Time, Speed, Throughput Capacity, Peeling efficiency, Tuber damage, Peeling weight proportion, percentage flesh loss respectively. The desirability for these optimization combinations ranges from 0.6 – 0.8. Figure 15 illustrate a 3D optimization graph for throughput capacity for developed machine. Figure 16 display a 3D optimization graph for peeling efficiency for developed machine. Figure 17 shows the 3D optimization graph for tuber damage for developed machine. Figure 18 illustrate a 3D optimization graph for peeling weight proportion for developed machine. Figure 19 display a 3D optimization graph for percentage flesh loss for developed machine. Table 12 shows the experimental results and predicted values of the responses from the model.

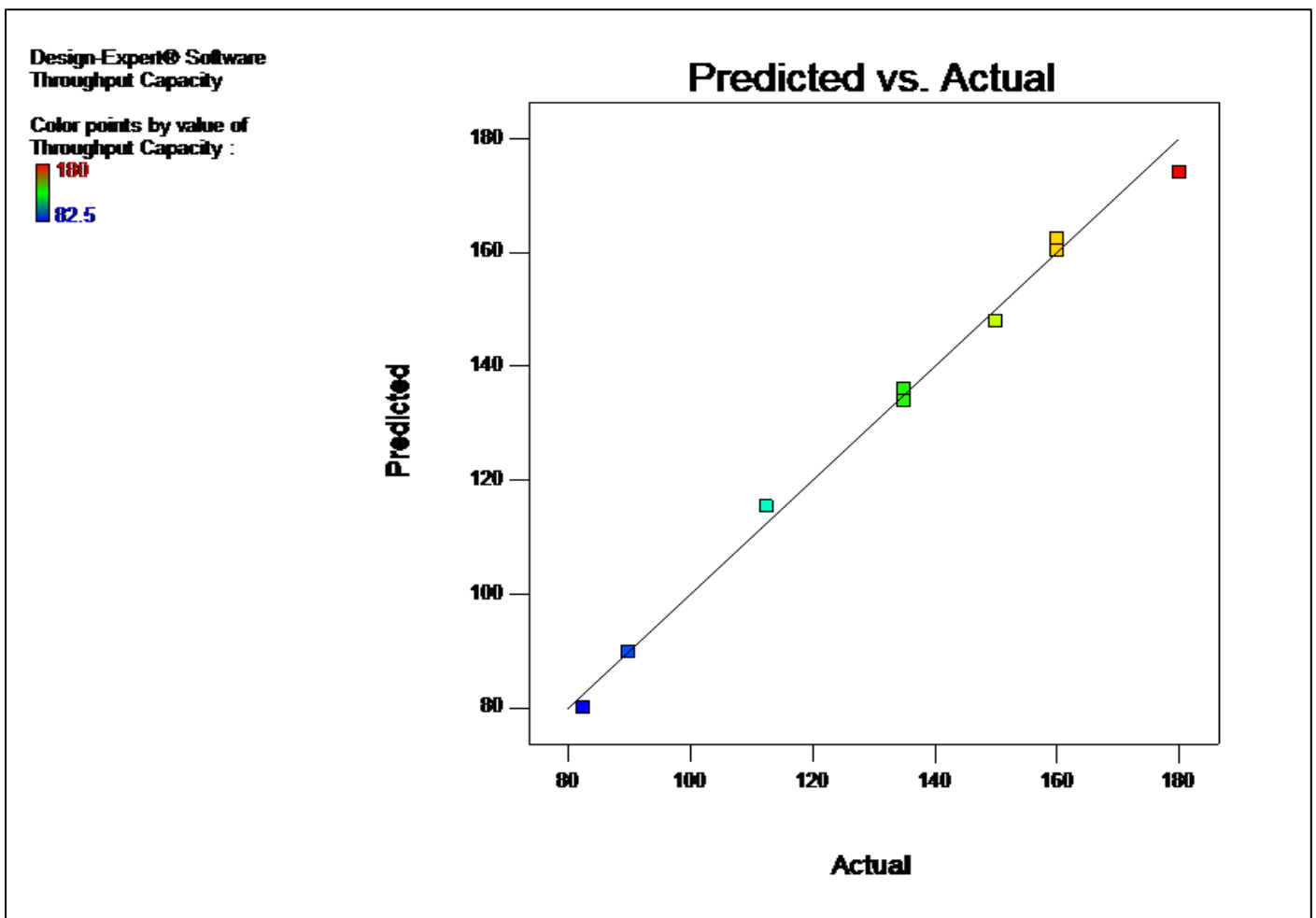


Fig 10: Diagnostics Graphs of Throughput Capacity

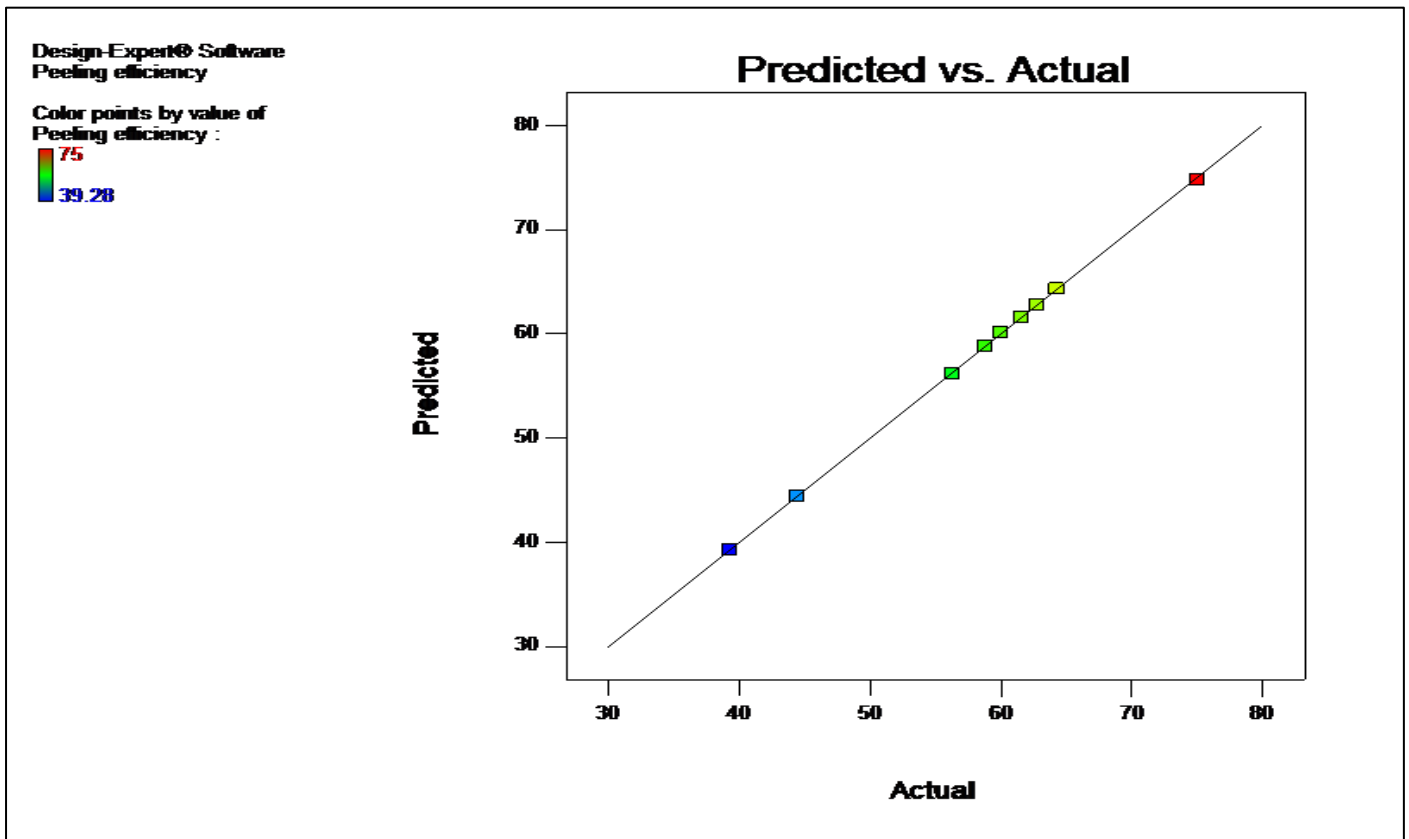


Fig 11: Diagnostics Graphs of Peeling Efficiency

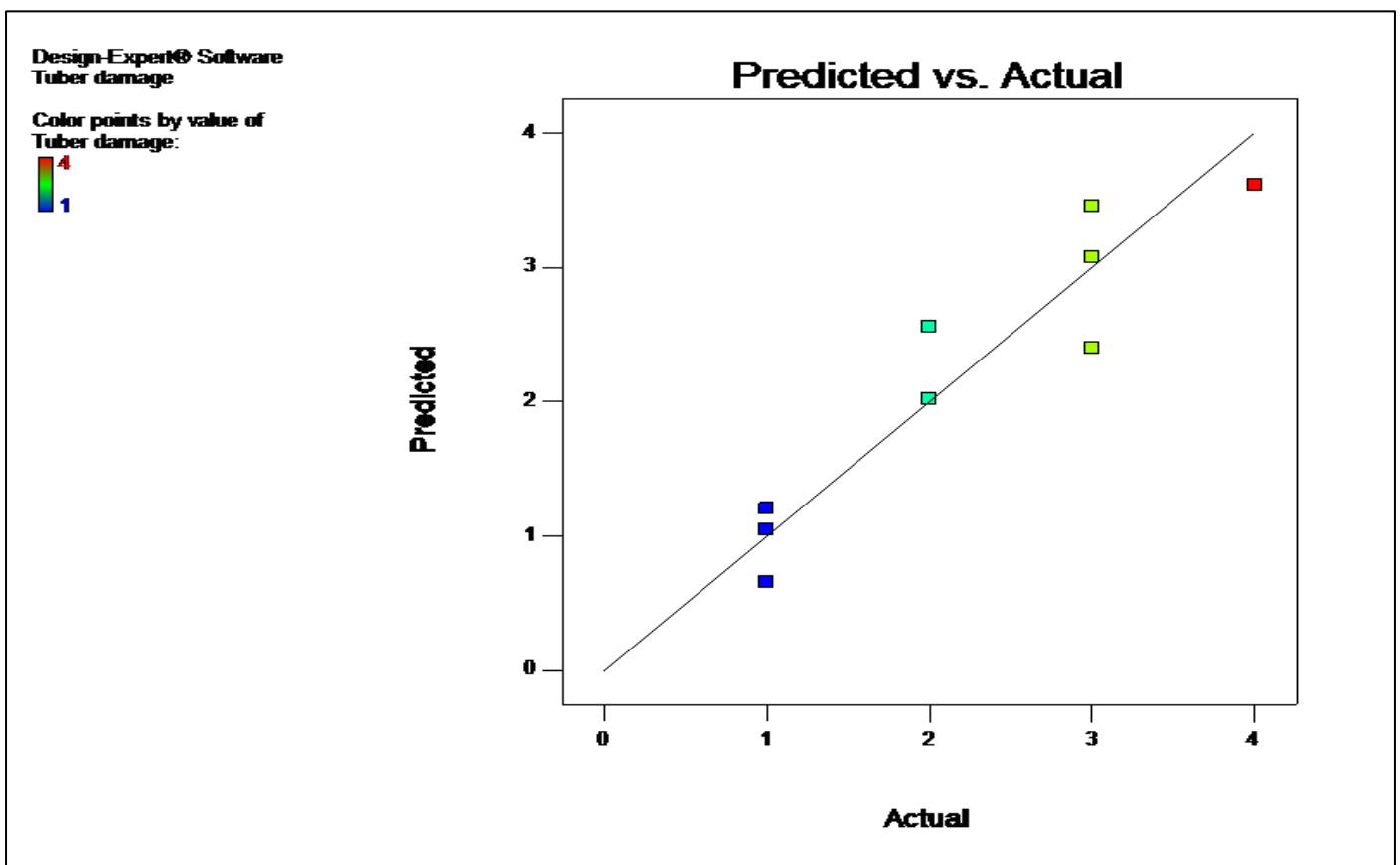


Fig 12: Diagnostics Graphs of Tuber Damage

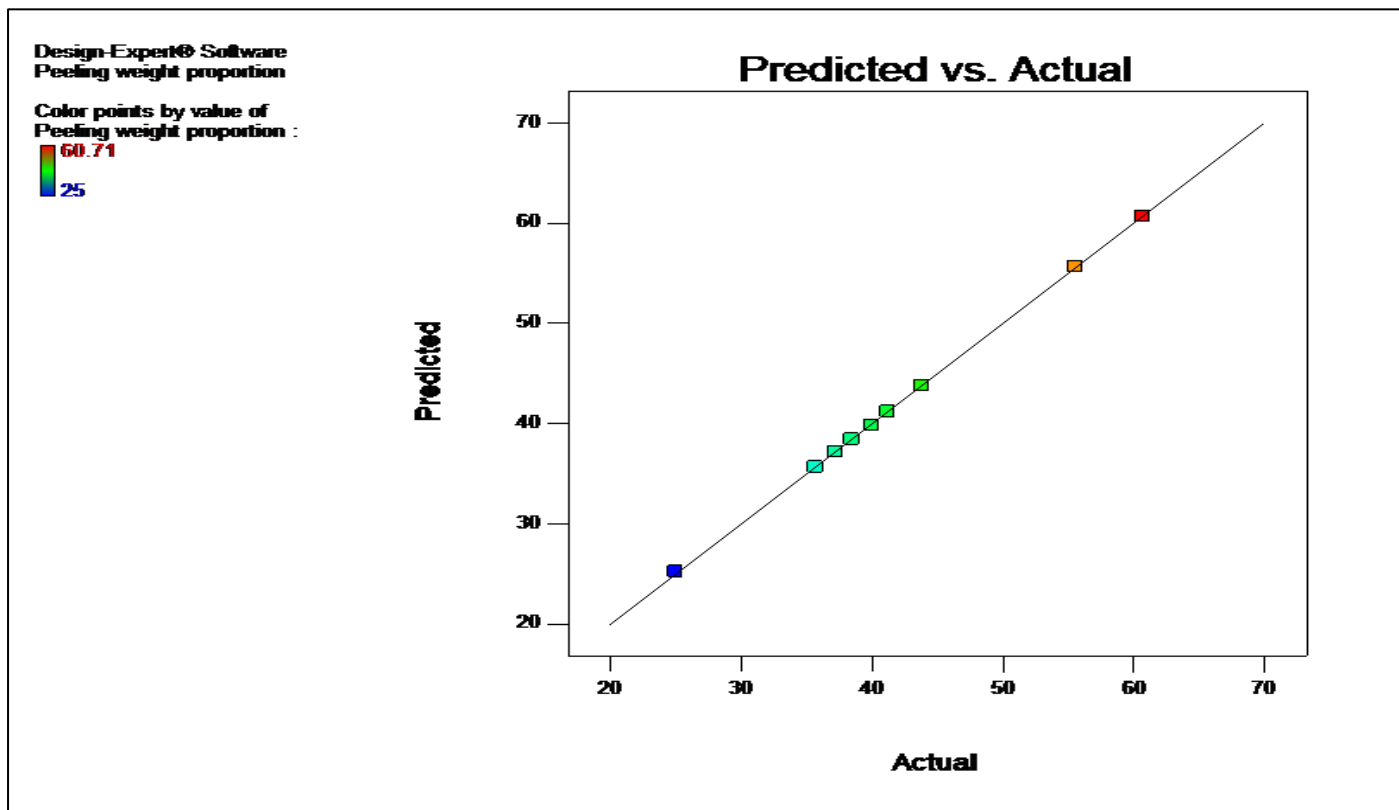


Fig 13: Diagnostics Graphs of Peeling Weight Proportion

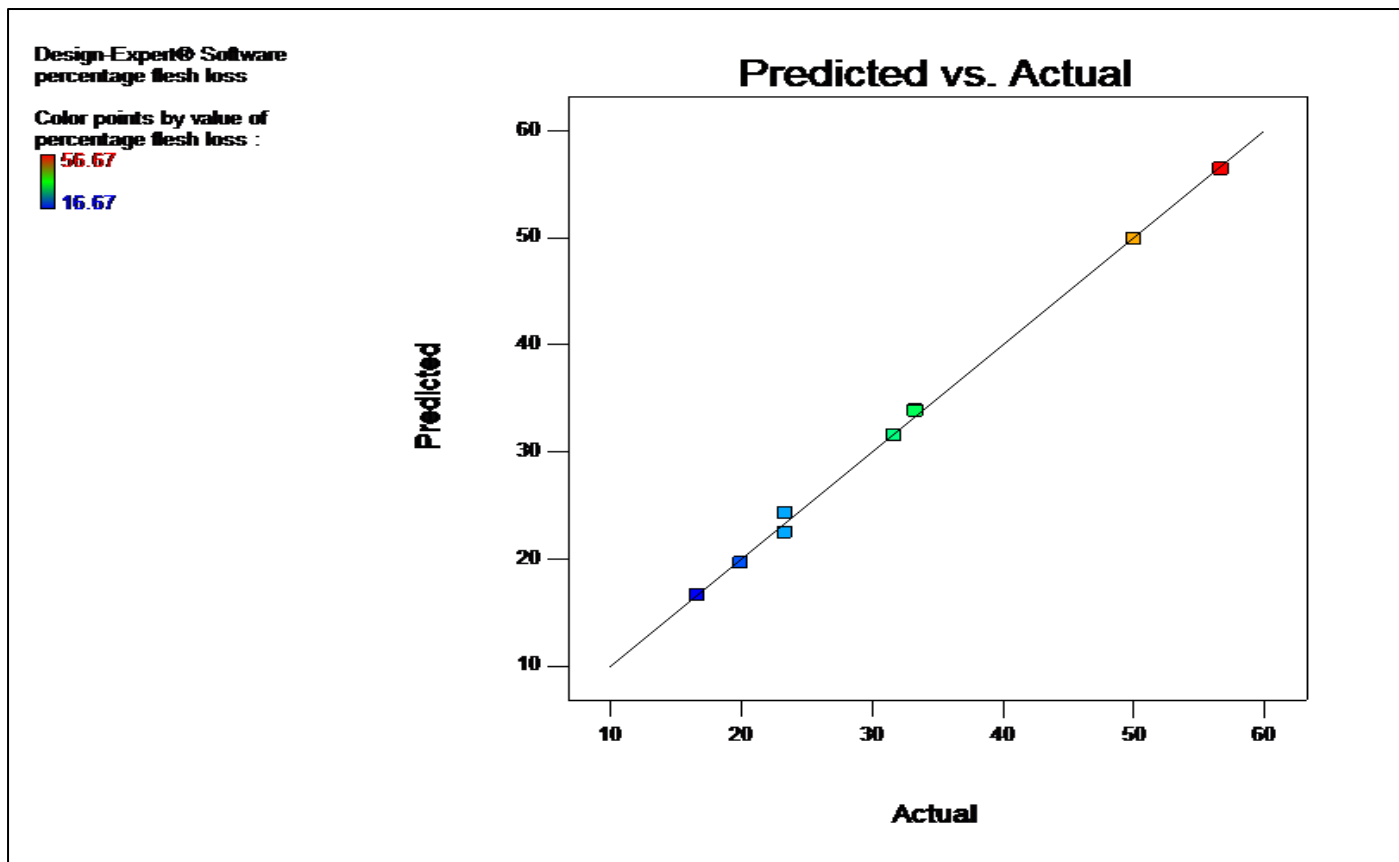


Fig 14: Diagnostics Graphs of Percentage Flesh Loss

Table 10: Optimization Constrain and Solutions for Operational Parameters of the Developed Cassava Peeling Machine

Constraints									
Name	Goal	Lower Limit	Upper Limit	Lower Weight	Upper Weight	Importance			
Time	in range	4	8	1	1	3			
Speed	in range	380	460	1	1	3			
Throughput Capacity	in range	82.5	180	1	1	3			
Peeling efficiency	maximize	39.28	75	1	1	3			
Tuber damage	minimize	1	4	1	1	3			
Peeling weight proportion	minimize	25	60.71	1	1	3			
percentage flesh loss	minimize	16.67	56.67	1	1	3			
Solutions									
Number	Time	Speed	Throughput Capacity	Peeling efficiency	Tuber damage	Peeling weight proportion	percentage flesh loss	Desirability	Desired choice
1	4.207	380	144.485	66.561	1.457	33.429	16.421	0.838	
2	4.23	380	145.356	66.793	1.501	33.197	16.404	0.838	
3	4.247	380	145.985	66.961	1.532	33.029	16.394	0.838	
4	4.262	380	146.559	67.114	1.56	32.876	16.385	0.838	
5	4.109	380	140.634	65.535	1.268	34.454	16.503	0.837	
6	4.331	380	149.029	67.774	1.685	32.216	16.353	0.837	
7	4.048	380	138.089	64.858	1.144	35.131	16.57	0.835	
8	4.544	380	155.974	69.635	2.046	30.356	16.338	0.828	
9	4	460	147.825	58.781	1.203	41.222	22.484	0.698	
10	4.05	460	149.366	59.155	1.305	40.847	22.632	0.697	
11	4.072	460	150.036	59.317	1.351	40.685	22.701	0.696	
12	6.3	380	171.422	74.156	3.523	25.839	21.048	0.606	<b>Selected</b>
13	7.356	380	144.776	67.577	3.122	32.422	28.036	0.602	

Table 11: Confirmation (Validation) Report for the Operational Parameters Models used for Optimization

Two-sided, Confidence = 95%, n = 1									
Factor	Level	Low Level	High Level	Std Dev	Coding				
Time	4.709	4	8	0	Actual				
Speed	380	380	460	0	Actual				
Response	Predicted Mean	Predicted Median	Experimental Observed	Std Dev	n	SE Pred	95% PI low	Data Mean	95% PI high
Throughput Capacity kg/h	160.6	160.6	160	2.633	1	2.957	154.013	137.813	167.189
Peeling efficiency %	70.881	70.881	71	0.109	1	0.122	70.609	59.069	71.153
Tuber damage	2.299	2.299	2	0.352	1	0.393	1.435	2.313	3.164
Peeling weight proportion %	29.11	29.11	29	0.106	1	0.119	28.846	40.926	29.375
percentage flesh loss %	16.414	16.415	16	0.532	1	0.597	15.084	31.251	17.745

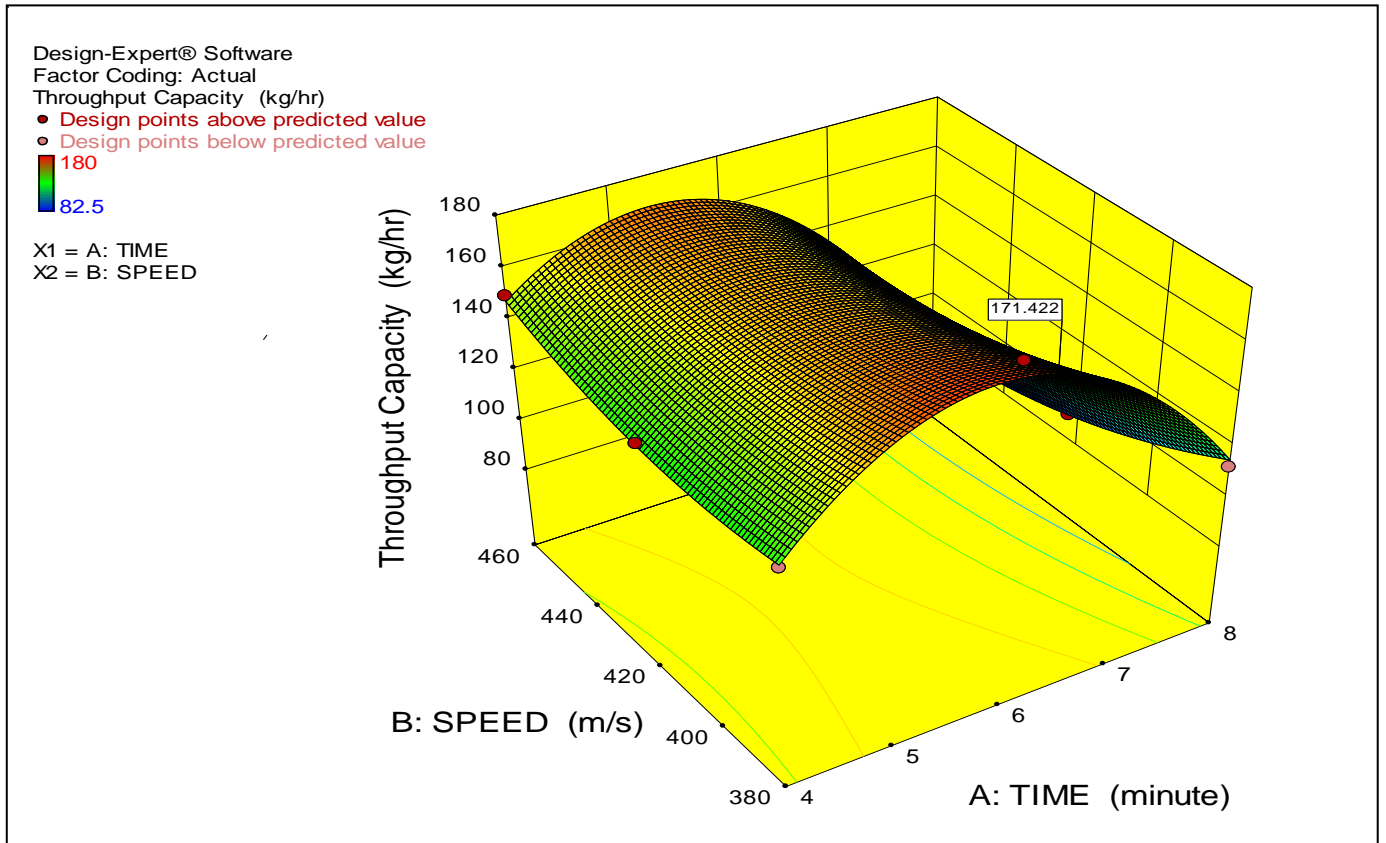


Fig 15: A 3D Optimization Graph for Throughput Capacity

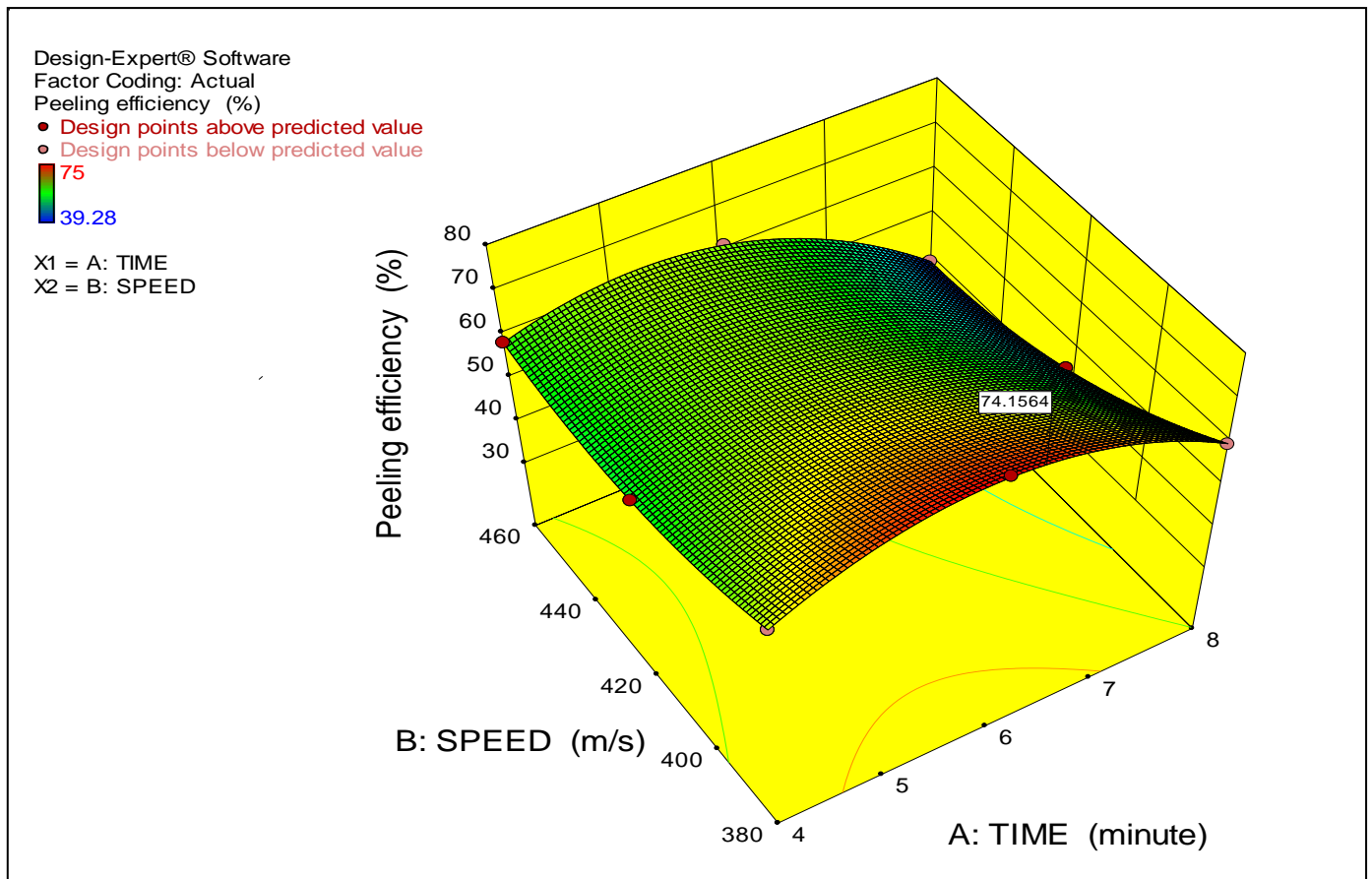


Fig 16: A 3D Optimization Graph for Peeling Efficiency

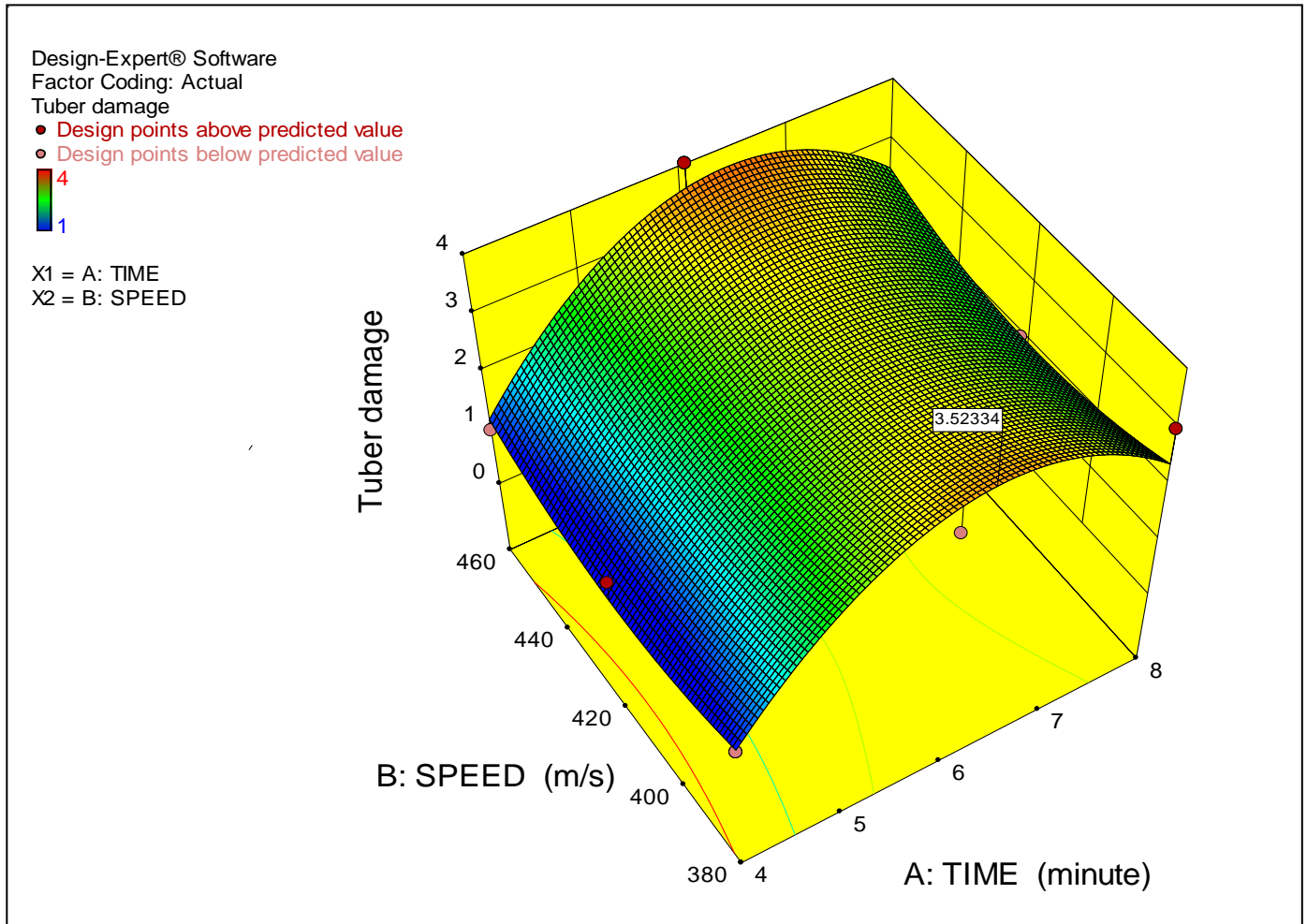


Fig 17: A 3D Optimization Graph for Tuber Damage

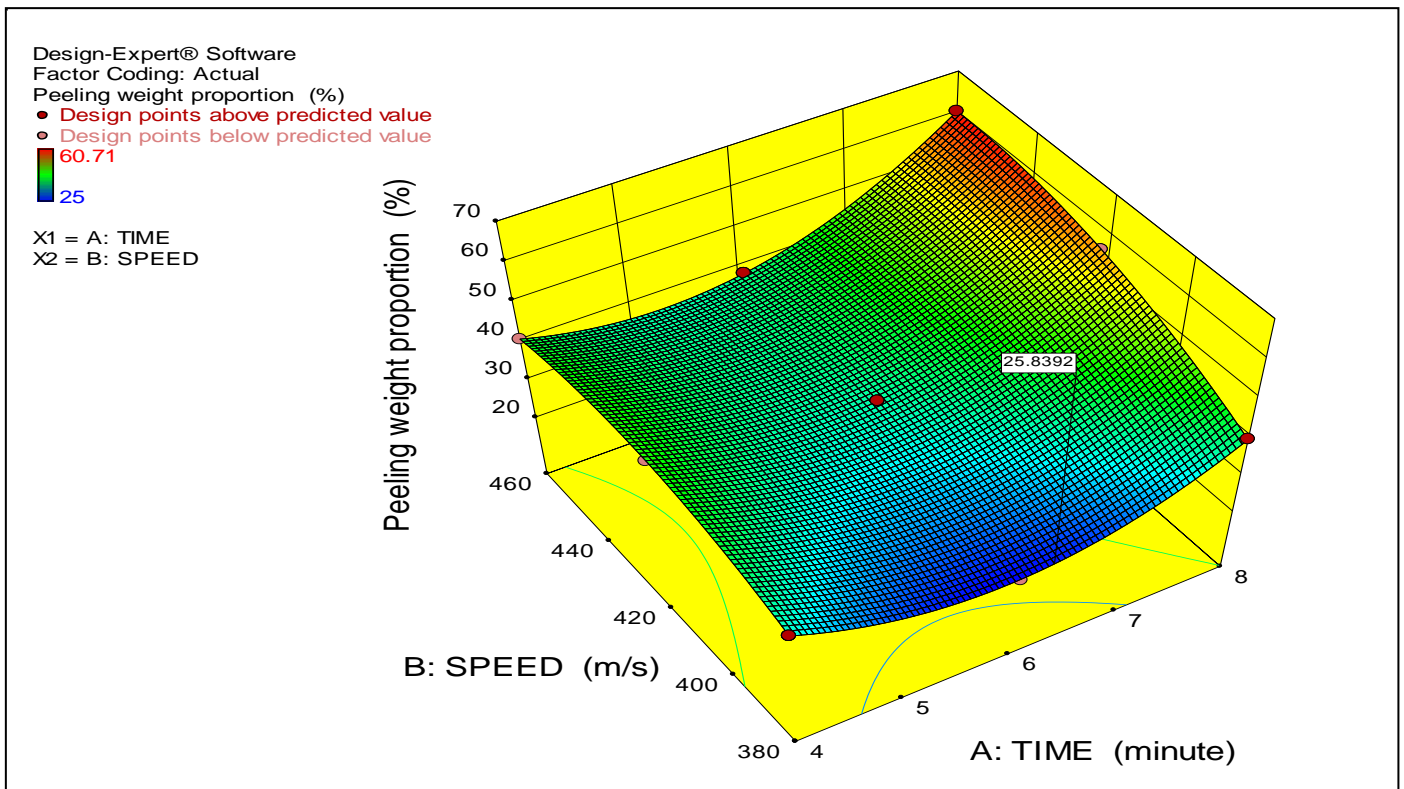


Fig 18: A 3D Optimization Graph for Peeling Weight Proportion

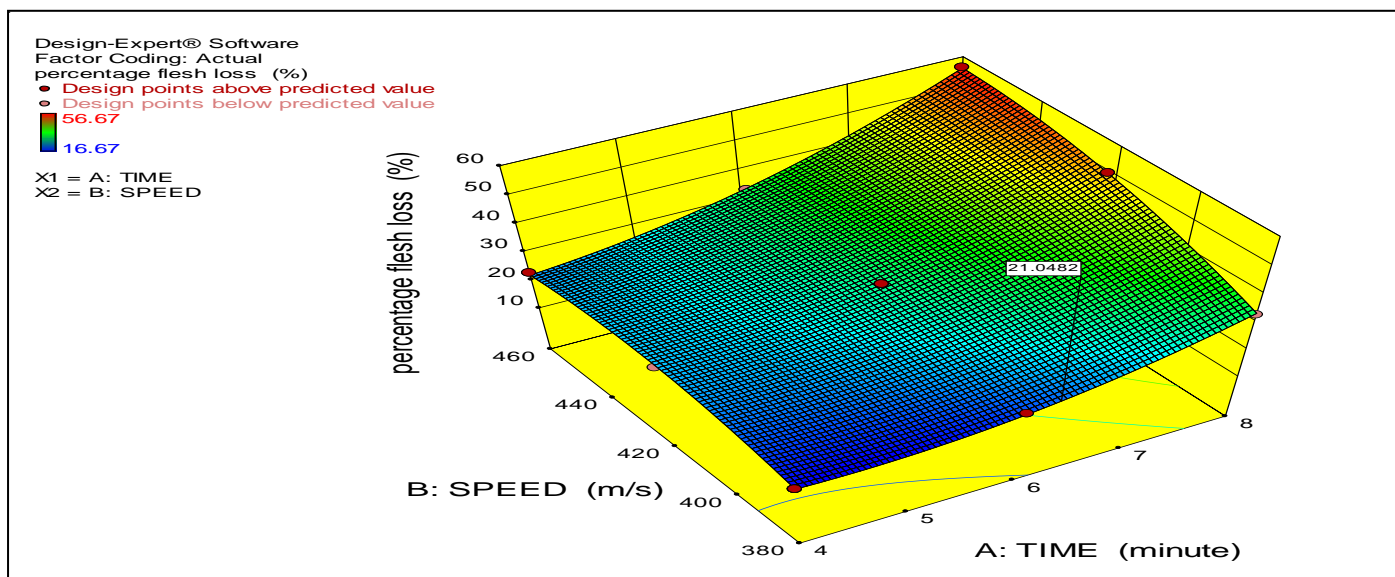


Fig 19: A 3D Optimization Graph for Percentage Flesh Loss

Table 12: The Experimental Results and Predicted Values of the Responses from the Models

S/ N	Mach ine speed, rpm	Peeli ng time, mins	Parameters							
			Peeling efficiency (%)				Percentage flesh loss of tubers (%)			
			Experimen tal	Predict ed	Percenta ge Deviatio n %	Coefficie nt of Variatio n, %	Experimen tal	Predict ed	Percenta ge Deviatio n %	Coefficie nt of Variatio n, %
1	100	2	55.14	55.46	0.58	0.41	1.01	1.13	11.88	0.713
2	100	4	60.09	59.87	0.37	0.26	2.20	2.19	0.45	0.002
3	100	6	66.05	64.28	2.68	1.89	3.27	3.25	0.61	0.006
4	200	2	69.71	68.86	1.22	0.86	4.12	4.23	2.67	0.147
5	200	4	72.20	73.27	1.48	1.05	5.51	5.29	3.99	0.439
6	200	6	74.28	77.68	4.58	3.24	6.51	6.35	2.46	0.197
7	300	2	81.61	82.26	0.80	0.56	7.53	7.33	2.66	0.266
8	300	4	87.35	86.67	0.78	0.55	8.34	8.39	0.60	0.015
9	300	6	92.59	91.08	1.63	1.15	9.24	9.45	2.27	0.239
Mean					1.57	1.11			3.07	0.225

**IV. DISCUSSIONS**

*A. Evaluation*

Table 6 show the result obtained from the evaluation of the cassava peeling machine. It was observed that throughput capacity, peeling efficiency, tuber damage, peeling weight proportion and percentage flesh loss of the peeling machine varied, depending on the speed of the peeling drum and the time of peeling. This variation could be attributing to so many factors. Like the irregular shape of cassava tubers, feeding rate, different sizes of tubers and the abrasive peeling material used. This variation in these operating parameters makes it mandatory to optimize the operating factors like time and speed that will achieve the desired operational parameters for optimum output. Similar variation in operational parameters for peeling cassava had been observed by other researchers like: Akintunde et al., 2005; Olukunle and Jimoh, 2012; Abdukadir, 2012; Olukunle and Akinnuli, 2013; Oluwole and Adio, 2013; Ukenna and Okechukwu, 2014.

*B. Modeling*

In other to optimize operational parameters of the developed cassava peeling machine, modeling of these parameters are necessary. Model analysis among the five types of models (linear, 2FI, quadratic and cubic) chosen show that quadratic model performed better; for all the operational parameters involved in this study (table 7). Quadratic model exhibit extremely low Sequential p-value which is the probability that the model terms are modeling noise (error) rather than helping explain the trend in the response. This means that quadratic model can explain the relationship or effect of the factors (time and speed) on the responses (throughput capacity, peeling efficiency, tuber damage, peeling weight proportion and percentage flesh loss) better than the other models. All the model type tested show no Lack of Fit p-value (the amount the model predictions miss the observations). This means that all types of model considered had high accuracy. Quadratic model also had a high Adjusted R-Square (measure of the amount of variation around the mean explained by the model, adjusted for the number of terms in the model) of 0.99 (99%). This Adjusted R-Square was higher in quadratic than the other types of

model expect in cubic. The cubic model was 'Aliased' meaning that there are not enough unique design points (number of experiments) to independently estimate all the coefficients for this model. Also quadratic model had a very high Predicted R-Square (measure of the amount of variation in new data explained by the model) of 0.99 (99%); in all responses modeled except in tuber damage which had a value of 0.55 (55%). This could be due to the fact that the number of damage tuber do not have unit of measurement unlike the other responses. After chosen quadratic models for all five responses in this study, the needs to know the degree of accuracy of the chosen model become necessary.

Analysis of variance (ANOVA) carried out on the quadratic equations for each response (operational parameter) used in this study; show that all terms in all the equations are significant at  $p < 0.05$  (table 8). This means that all terms used in the quadratic equations had a great impact in predicting the operational parameters of the cassava peeling machine. The ANOVA analyses also show that the quadratic models developed had no lack of fit. This means the error in predicting the operating parameters is zero. Indicating great accuracy in the quadratic models developed. Now that ANOVA had showed that the models developed are accurate with great impact on the predicting outcome. Let us now examine to what extent are these accuracies and how precise are these models.

The statistical analysis of the quadratic models (table 9) shows that their standard deviations are less than zero; Except for throughput capacity which is 2.632. This means that power in predicting the other operating parameters or responses are slightly more accurate than that of the throughput capacity. This occurrence may be due to experimental error. The coefficient of variation of the quadratic models developed were all low (less than 2), except for damage tuber model which is 15.2%. Coefficient of variation shows how frequent a model will predict an exact number. This is a measurement of precision. This then means that all the operating parameters models are more precise than that of damage tuber. This occurrence could be due to the data distribution of the experimental data collected. The PRESS (Predicted Residual Sum of Squares) of the model which is a measure of how well a particular model fits each point in the design. This is a measure of cross-validating if the model is accurately describing the relationship between the factors (time and speed) and the responses (operational parameters). All equations developed had lower PRESS (less than 20) except for throughput capacity which had 394. This indicates that the structures of all the developed equations are more valid or better than that of throughput capacity. This occurrence means that the throughput capacity equation is

over fitted. The -2 Log Likelihood (the coefficient estimates for the chosen model to maximize the likelihood that the fitted model is the correct model) is a measure of goodness fitness or variance for the model. Peeling efficiency model had the lowest value of -2 Log Likelihood while the throughput capacity had the highest value. This means that in term of overall performance the peeling efficiency model is the best while the throughput capacity model is the least. The R-Squared (measure of the amount of variation around the mean explained by the model), Adj R-Squared (measure of the amount of variation around the mean explained by the model, adjusted for the number of terms in the model) and Pred R-Squared (measure of the amount of variation in new data explained by the model); of all quadratic equations developed are greater than 0.9 (90%) except for damage tuber equation. Damage tube equation had an Adj R-Squared of 0.89 (89%) an Pred R-Squared of 0.77 (77%). This means that predictive capacity is lower in the damage tube developed equation than for the other developed equations. These occurrences can also be attributed to the distribution of the collected experimental data. Adequate Precision which is a signal-to-noise ratio is greater than 4 for all quadratic equation developed. Ratios greater than 4 indicate adequate model discrimination. This shows that all the equations had good precision and can be used for calibration. Peeling efficiency and percentage weight model equations had the best precision (above 500). The BIC (a large design penalized likelihood statistic used to choose the best model) and AICc (a small to medium penalized likelihood statistic used to choose the best model). These are just calculated parameters used to stop or reduce the terms in the models if they become too much or too little to cause the model equation to over fit or under fit. BIC (Bayesian information criterion) is used by the equations when the experimental data becomes very large. AICc (Akaike information criterion) is used by the equations when the experimental data becomes very small. After looking at the properties of the model equations, we need to diagnose the equations to see if the experimental data need transformation or not.

Transformation of data is done when model equation is performing poorly. Even though our model equation had performed well, nevertheless the need to diagnose is necessary. Diagnostic graphs of predicted against actual experimental data were plotted if figure 10. The graphs of all developed quadratic equations developed show a constant variance along the graph. This is good because it shows that experimental data are evenly distributed. If there were expanding variance ("megaphone pattern <") in these plots, this will indicates the need for a transformation. Now let that a look at the structure of the developed model equations

➤ *The Quadratic Model Equations Developed are Shown Below:*

$$\bullet \text{ Throughput capacity} = 349.426 + 195.874 T - 3.394 S - 0.147 TS - 12.096 T^2 + 4.916S^2 \quad (1)$$

$$\bullet \text{ Peeling Efficiency} = 507.174 + 54.719 T - 2.691 S - 0.048 TS - 3.137T^2 + 3.349 \times 10^{-3} S^2 \quad (2)$$

$$\bullet \text{ Tuber Damage} = 35.7 + 5.548 T - 0.241 S - 0.434T^2 + 2.898 \times 10^{-4} S^2 \quad (3)$$

$$\bullet \text{ Peeling Weight Proppotion} = -407.085 - 54.697 T + 2.67 S + 0.048 TS + 3.131T^2 - 3.347 \times 10^{-3} S^2 \quad (4)$$

$$\bullet \text{ Percentage Flesh Loss} = -422.055 - 32.384 T + 2.353 S + 0.052 TS + 1.398T^2 - 2.964 \times 10^{-3} S^2 \quad (5)$$

The confirmation (Validation) of these developed models was done using new performed experimentally data (table 11). The 95% PI (Prediction Interval) is statically calculated and used as a test tool to test if the experimental results gotten from the confirmatory experiment lies between the calculated 95% PI low and 95% PI high. Levels of factors that were used for the confirmatory test were calculated by the software (Design Expert). The confirmatory result shows that all operational parameter (throughput capacity, peeling efficiency, tuber damage, peeling weight proportion and percentage flesh loss) values gotten in the confirmatory test; all lies within the 95% prediction intervals. This shows that the developed models equations are performing as it was design to perform. All confirmatory tests for each operational parameter were carried out once as specified by the software. This is because of the high confidence level used by the software.

#### C. Effect of Time and Speed on the Operational Parameters of the Developed Machine

Analysis of variance (ANOVA) shows that speed, time and its interactions are significant to all the operational parameters at  $p < 0.05$  (table 8). This is due to the irregular shapes and sizes of the cassava tubes. The real behaviors of all the operational parameters with speed and time are illustrated in figures 15 – 19.

In figure 15, as time of operation increases the throughput capacities increases to a maximum point and then start decreasing. This means that at this maximum point, all the cassavas had been peeled and fresh loss is taken place. This exact maximum point can only be known by optimizing the throughput capacity with time. Also the speed of the machine is increases the throughput capacity decreases to a point and then it start increasing again. This phenomenon occurs because continuous increment of speed causes the cassava tubers to break due to high impact of the cassava on the peeling drum. This in turn reduces the throughput capacity. The sudden increments of throughput capacity as speed continuously increases; could be as a result that the rotating peeling drum is realigning the cassava tuber position for effective peeling. Similar observation had been noted by Oluwole and Adio, 2013; Olukunle and Akinnuli, 2013. So the need to know the right point to fine tune speed to get the best throughput requires optimization.

The peeling efficiency has similar behavioral trend as the throughput capacity with time and speed (figure 16). This increase and decrease in peeling efficiency with time and speed can also be explained using the explanations given for throughput capacity. Also to get the best peeling efficiency in this fluctuation behavior requires optimization. Similar peeling efficiency behavior had been reported by Adetan et al.; 2003 and Olukunle; 2005 and Jimoh *et al.* 2014.

The damage tubes increases as the time of operation increases to a maximum point and then start reducing (figure 17). This occurrence could be because at the maximum point, all the cassava tubes had been peel and there is less shear stress on the cassava tubes. The continuous increase in speed increases the numbers of tubers damaged. This trend shows

that the increase in speed increases the shear force applied to the tuber during peeling. To get the best speed and time for less tuber damage requires optimization.

Peeling weight proportion decreases as time of operation increases to a certain point and then start increasing after that point (figure 18). This could be explained from the view that as the time of operation continues some part of the cassava tubers could not be peeled. Then after so time the orientation of the tubers are changed by the action of the peeling drum to cause further peeling. Also as the speed of the machine increases in peeling weight proportion increases. This occurs because increase in speed continuously will cause the machine to start peeling the cassava flesh as well. Some researchers that had observed similar trends includes: Asoegwu, 1981; Odigboh, 1983a; Igbeka, 1980, 1984, 1985; Nanda and Matthew, 1996; Nwagugu and Okonkwo, 2009; Sajeev et al., 2009.

Percentage flesh loss increases with increase in time of operation (figure 19). This could be explained from the view that; as the machine continue in operation the area that had been already peeled, will come in contact with the abrasive surface of the peeling drum to cause continuous flesh loss. Also the percentage flesh loss increases with increase in speed of the machine. This occurs because as the speed of the machine is increased the shear stress on the peeling tubers increases causing more flesh of the cassava to be lost. To find the right speed and time to reduce the percentage flesh loss, the percentage flesh loss parameter need to be optimized.

#### D. Optimization of the operating parameters of the developed cassava peeling machine

To optimize the operating parameters certain desired goals or constrain are chosen (table 10). These goals are:

- To find out the best time within the range of time used in this study to achieve desired operating parameters.
- To find out the best operating speed within the range of speed used in this study to achieve desired operating parameters
- To determine the best throughput capacity within the ranged of experimented throughput values.
- To determine the maximum peeling efficiency
- To determine the minimal damage tuber
- To determine the minimal Peeling weight proportion
- To determine the minimal percentage flesh loss

After setting the goals or constrain, the solutions obtain by the software are displayed in table 10. The maximum peeling efficiency of 74% was achieved at the speed of 380m/s, when the machine had operated for 6min. This point was also displayed as flag on figure 16. At this optimal efficiency the machine had an optimal throughput of 171.4kg/h. This point was also displayed as flag on figure 15. The minimum optimal damage tubers at this optimal peeling efficiency are 3.3 tubers (figure 17). Also at this optimal peeling efficiency the minimum optimal peeling weight proportion was 25.8% (figure 18). Final at this optimal peeling efficiency the optimal percentage flesh loss was at 21% (figure 19). These were the best results when

considering the efficiency of the developed cassava peeling machine. The desirability (an objective function that ranges from zero outside of the limits to one at the goal) of all these optimal values obtained with the maximum peeling efficiency was 0.6 (60%). This means that optimal values obtain meet 60% of the goal of the optimization. Nevertheless other solutions can also be formulated from this analysis.

An optimal minimal flesh loss of 16.3% was achieved at a speed of 380m/s when the machine is allowed to operate for 4.5 minutes (table 10). The optimum peel efficiency here was 69.6%. Optimum throughput was 156kg/h with an optimal tubers damage to be 2 tubers. The optimal peeling weight proportion was 30%. The desirability (an objective function that ranges from zero outside of the limits to one at the goal) of all these optimal values obtained with the minimal flesh loss was 0.83 (83%). This means that optimal values obtain meet 83% of the goal of the optimization. These two optimum solutions can be recommended to the end users of the developed cassava peeling machine.

## V. CONCLUSION AND RCOMMENDATION

### A. Conclusion

A cassava peeling machine was design and constructed. Evaluation was carried out on this developed cassava peeling machine. The operational parameters used in evaluation were modeled. Quadratic models were developed, tested and confirmed to be the best models for optimizing the operational parameters. The operational parameters were optimized and two optimum solutions were proposed for end user.

### B. Recommendations

- It is recommended that cutting of the tubers should be made at regions where there are very close diametric dimensions to facilitate better peeling and minimize manual finishing,
- The machine should be operated with the machine speed of 380 rpm and peeling duration of 6 minutes for optimum performance,
- The effects of factors such as varieties of cassava, moisture content and brush types on peeling performance should be investigated,
- The machine should be used to test other roots and tubers like potatoes and cocoyam.

## REFERENCES

- [1]. Abdulkadir, B.H. (2012). Design and fabrication of a cassava peeling machine. International Organization on Scientific Research (IOSR). *Journal of Engineering (IOSRJEN)*, 2(6): 01-08.
- [2]. Adetan, D.A., Adekoya, L.O. and Aluko, O.B. (2003). Characterization of some properties of cassava root tubers. *Journal of Food Engineering*, 59: 349-353.
- [3]. Adetan, D.A., Adekoya, L.O. and Aluko, O.B. (2006). Theory of mechanical method of peeling cassava tubers with knives. *International Journal of Agrophysics*, 20: 269-276.
- [4]. Adetan, D.A., Adekoya, L.O., Aluko, O.B. and Mankanjuola, G.A. (2005). An experimental mechanical cassava tubers peeling machine. *Journal of Agriculture Engineering and Technology (JAET)*, 13(4): 67-69.
- [5]. Adetunji, O.R. and Quadri, A.H. (2011). Design and fabrication of an improved cassava grater. *Pacific Journal of Science and Technology*, 12(2): 120-129.
- [6]. Akintunde, B.O., Oyawale, F.A. and Tunde-Akintunde, T.Y. (2005). Design and fabrication of a cassava peeling machine. *Nigerian Food Journal*, 23: 1 - 8.
- [7]. Asoegwu, N.S. (1981). Determination of some mechanical properties of cassava root: *Manihot Esculenta Cranz*, Unpublished M.Sc. Thesis. University of Ife, Ile-Ife, Nigeria.
- [8]. FAO (1999). Accessed 15 January, 2015, from [www.fao.org](http://www.fao.org)
- [9]. FAO (Food and Agricultural Organization). (2005). Storage and Processing of Roots and Tubers in the Toopies, Agriculture and Consumer Production.
- [10]. Igbeka, J.C. (1980). Relationship of moisture diffusivity with moisture content and temperature in cassava (*Manihot Esculenta Cranz*) and potato (*Solarum tuberosum*) during drying. *Nigeria Journal of Science*, 14: 27 – 36.
- [11]. Igbeka, J.C. (1984). Some mechanical and rheological properties of yam and cassava. *African Journal of Science and Technology*, 3(2): 45-60.
- [12]. Igbeka, J.C. (1985). Mechanization of tuber (cassava) peeling. Proceedings of the International Symposium on Mechanization of Harvesting and Subsequent Processing of Agricultural Products in Tropical Africa and the Manufacturing of Relevant Agricultural Implements Yaounde, Cameroon, 410-422.
- [13]. Jimoh, M.O., Olukunle, O.J. Manuwa, S.I. and Amumeji, O.T. (2014). Theoretical analysis of tuber movement during mechanical peeling of cassava. International Organization on Scientific Research (IOSR). *Journal of Mechanical and Civil Engineering (IOSR-JMCE)* 11, 6(1); 27-36.
- [14]. Khurmi, R. S. and Gupta, J. K. (2008). A textbook of machine design, 14th edition. New Delhi: Eurasia Publishing House (PVT) Limited, Ram Nagar, India, 1230 pp.
- [15]. Kolawole, O.P., Agbetoye, L.A.S. & Ogunlowo, A.S. (2010).Sustaining world food security with improved cassava processing technologies: *The Nigerian Experience on Sustainability*, 2; 3681- 3694.
- [16]. Nanda, S. K., and Mathew, G. (1996). Physical aspects of softening of cassava tubers upon fermentation with a mixed culture inoculums. *Journal of Food Engineering*, 29: 129 – 134.
- [17]. Ndirika V.I.O and Oyeleke, O.O. (2006). Determination of Selected Physical Properties and their Relationship with moisture Content for Millet. *Applied Engineering in Agriculture*, 22(2): 291-297.

- [18]. Nwachukwu, I.D, and K. J. Simonyan . 2015. Some Engineering Properties of Cassava Tuber Related To Its Peeling Mechanization. *Umudike Journal of Engineering and Technology (Ujet)*, Vol. 1, No. 1, 12-24.
- [19]. Nwagugu, N.I., and Okonkwo, W.I. (2009). Experimental determination of comprehensive strength of sweet cassava (*Manihot Esculenta* Cranz). *International Conference of West African Society of Agricultural Engineers and Nigerian Institution of Agricultural Engineers*, 9 – 197.
- [20]. Odigboh, E.U. (1983a). Cassava production, processing and utilization, In: Chan Jnr, H. T. (ed.), *Handbook of Tropical Foods*, New York: Merce Decker Pub. Inc., 145-200.
- [21]. Olukunle, O.J. (2005). Development of a cassava peeling machine. Abstract, Proceedings of the International Conference on Global Food and Product Chain Dynamics, Innovations, Conflicts and strategies, 'Tropentag 2005', University of Hohenheim Stuttgart, Germany, 54.
- [22]. Olukunle, O.J. and Akinnuli, B.O. (2013). Theory of an automated cassava peeling system. *International Journal of Engineering and Technology (IJEIT)*, 2: 2277-3754.
- [23]. Olukunle, O.J. and Jimoh, M.O. (2012). Comparative analysis and performance evaluation of three cassava peeling machines. *International Research Journal of Engineering Science, Technology and Innovation (IRJESTI)*, 1(4): 94-102.
- [24]. Olukunle, O.J. and Jimoh, M.O. (2012). Comparative Analysis and Performance Evaluation of Three Cassava Peeling Machines. *International Research Journal of Engineering Science, Technology and Innovation (IRJESTI)*, 1(4): 94-102.
- [25]. Sajeev, M.S., Sreekumar, J. Unnikrishnan, J. Moorthy, M.S.N. and Shanavas, S. (2009). Kinetics of thermal softening of cassava tubers and rheological modeling of the starch, *Journal of Food Science and Technology*, 47(5): 507-518.
- [26]. Ukenna, R.U. and Okechukwu, V.J. (2014). Development and modification of cassava peeling and washing machine.
- [27]. Agricultural Engineering Department, B. Eng. Thesis. Federal University of Technology Owerri (FUTO), Nigeria.
- [28]. Uthman, F. (2011), Design and fabrication of cassava lump breaking and sieving machine. *Oasis Journal of Research and Development*, 1(2): 42-50.